Aus dem Institut für Pharmakologie und Toxikologie
Geschäftsführender Direktor: Prof. Dr. med. Thomas Gudermann
des Fachbereichs Medizin der Philipps-Universität Marburg

Characterization of mouse polycystic kidney disease and receptor for egg jelly gene and protein in heterologous and native system

Inaugural-Dissertation
zur Erlangung des Doktorgrades
der Humanbiologie
(Dr. rer. physiol.)

dem Fachbereich Medizin
der Philipps-Universität Marburg
vorgelegt

von
Yulia Butscheid geb. Gantievskaya
aus Minsk / Belarus

Marburg 2006

Angenommen vom Fachbereich Medizin der Philipps-Universität Marburg am 24.03.2006.

Gedruckt mit der Genehmigung des Fachbereichs.

Dekan: Prof. Dr. med. Bernhard Maisch
Referent: Prof. Dr. Thomas Gudermann
Koreferent: Prof. Dr. Dr. Jürgen Daut

For my parents Tamara and Alexander

For my husband Moritz

TABLE OF CONTENTS

1. INTRODUCTION

1.1. Male gametes

The spermatozoon is the end product of gametogenesis in the male, which occurs within the seminiferous tubules of the testis. This process involves a series of mitotic divisions of spermatogonia stem cells, two meiotic divisions by spermatocytes, extensive morphological remodelling of spermatids during spermiogenesis, and the release of free cells into the lumen of the seminiferous tubules by spermiation.

1.1.1. Morphology of mammalian spermatozoa

Spermatozoa of all mammals have two main components, the head and the flagellum or tail, which are joined at the neck. The head consists of the acrosome, the nucleus, and only small amount of cytoskeleton structures and cytoplasm. The acrosome is a membrane organelle containing hydrolytic enzymes that are released during the acrosome reaction. The sperm flagellum has a central axoneme surrounded by outer dense fibers extending from the head to near the posterior end. Mitochondria are around the dense fibers in the anterior part of the flagellum and a fibrous sheath in its posterior part. The flagellum, like the head, is tightly wrapped by the plasma membrane and contains little cytoplasm.

Although all mammalian spermatozoa have these general characteristics, there are species-specific differences in the size and shape of the head and the length and relative size of the components of the flagellum. Sperm of most mammalian species have a spatulate head, the nucleus and acrosome are flattened in the plane of the anterior-posterior axis of the sperm and they are usually symmetric. However, in some animals, protrusions of the acrosome extend perpendicular by the flattened plane of the sperm head. Thus, rodent sperm usually have a falciform-shaped head, with the acrosome overlying the convex margin of the nucleus.

1.1.2. Domain organisation of the sperm plasma membrane

The unique feature of the spermatozoon is that the plasma membrane is subdivided into well-defined regional domains that differ in composition and function. These domains are dynamic structures and can undergo changes during the life of the

cell. The major domains of the sperm head plasma membrane in most mammals are the acrosomal and the postacrosomal regions. The first one includes the acrosomal cap and equatorial segment that may be separated by the central crescent (Fig. 1.1.). The acrosomal cap is more extensive in sperm with a spatulate head, such as those of humans, whereas the equatorial segment is larger in sperm with a falciform head like in mouse. The postacrosomal region includes the plasma membrane between the posterior margin of the acrosome and the posterior ring, which forms the junction between head and tail. The plasma membrane of the flagellum is separated into middle piece domain overlying the mitochondrial sheath and the principal piece.

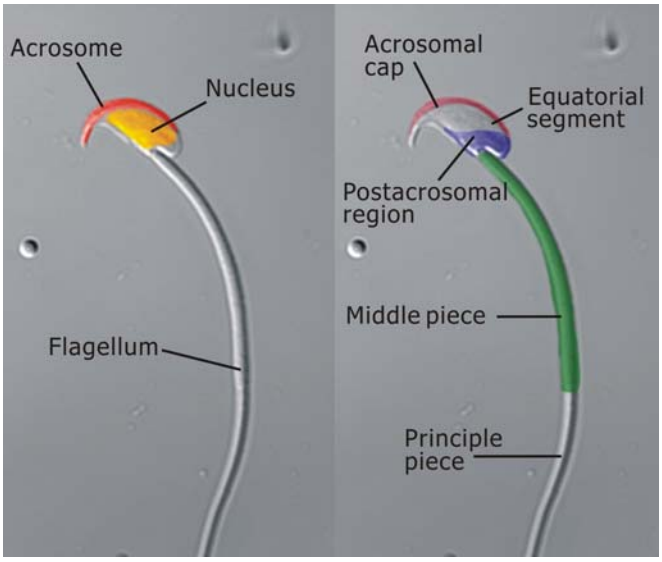

Figure 1.1. Morphology of mouse spermatozoon
(A) Structural components of the mouse spermatozoon; **(B)** Sperm plasma membrane domains.

1.1.3. Epididymal sperm maturation

Spermatozoa leave the testis neither fully motile nor able to recognize or fertilize an egg. To attain the capacity to fertilize, sperm undergoes many maturational changes during their transit in the epididymal duct (Yanagimachi, 1994). Functional changes occur in metabolic processes, the pattern and effectiveness of flagellar activity, and the ability to bind to the zona pellucida. Changes in plasma membrane composition and organisation contribute to these functional modifications. They are reflected by changes in surface charge, lectin binding, lipid and protein composition, protein glycosylation patterns, unmasking of some epitopes for antibody binding and etc. Other changes include alterations in the outer acrosomal membrane, gross morphological changes in acrosome in some species, and cross-linking of nuclear protamines and proteins of the outer dense fiber and fibrous sheath (Toshimori, 2003; Yanagimachi, 1994).

In mammals, the transit of spermatozoa through the epididymis usually takes 10-13 days, whereas in humans the estimated transit time is 2-6 days (Amann and

Howards, 1980; Johnson and Varner, 1988). The epididymal segment where most spermatozoa attain their full fertilizing capacity appears to be the proximal cauda. Spermatozoa from this region are capable of moving progressively, which is characteristic of spermatozoa preceding fertilization, and bind to zona-free hamster ova in vitro at a higher percentage than spermatozoa obtained from more proximal locations (Turner, 1995; Yanagimachi, 1994). The cauda epididymidis (and ductus deferens) are also regions where spermatozoa are stored before ejaculation (Jones, 1999; Turner, 1995). When ejaculation occurs, stored spermatozoa with the surrounding fluid are mixed with the alkaline secretions of the male accessory sex glands and deposited in the vagina.

1.1.4. Sperm capacitation

When spermatozoa first enter the female reproductive tract they are not capable of fertilization, although they are motile and appear to be morphologically mature. In vivo, ejaculated sperm require a finite period of residence in the female reproductive tract to become fertilization-competent. In 1951, Chang and Austin discovered that mammalian sperm must be activated, or capacitated, within the female reproductive tract to fertilize eggs. This time-dependent acquisition of fertilization competence has been defined as “capacitation”. The definition of capacitation has been modified over the years to include the acquisition of the ability of the acrosome-intact sperm to undergo the acrosome reaction in response to its interaction with the zona pellucida (Ward and Storey, 1984). Capacitation includes a variety of changes in the sperm plasma membrane (protein tyrosine phosphorylation, intracellular ions, metabolism, adenylate cyclase-cAMP system), nucleus, and acrosome (Fraser, 1995; Visconti et al., 1995a; Visconti et al., 1995b; Yanagimachi, 1994), but the exact mechanisms of capacitation in vivo remain a mystery.

Cauda but not caput epididymal sperm can undergo capacitation in vitro when incubated in balanced salt solution containing appropriate concentrations of electrolytes, metabolic energy and protein sources. Certain components of this medium such as serum albumin (Go and Wolf, 1985), Ca^{2+} (Coronel and Lardy, 1987; Fraser, 1987; Ruknudin and Silver, 1990; Yanagimachi, 1984) and HCO_3^- (Boatman and Robbins, 1991; Lee and Storey, 1986; Neill and Olds-Clarke, 1987) are absolutely required for capacitation. The time necessary for capacitation varies among species; in mouse, for

example, it is about 60-90 minutes. As a result of capacitation, sperm have an altered pattern of motility (called hyperactivation) and are capable of undergoing the acrosome reaction.

1.1.5. Acrosome reaction

The functional significance of the acrosome reaction (AR) is to render spermatozoa capable of penetrating through the zona pellucida and fusing with the egg plasma membrane. The acrosome reaction is a Ca^{2+}-stimulated exocytosis involving reorganization of the membranes in the head of the spermatozoon. Multiple fusions occurring between the outer region of the acrosomal membrane and the plasma membrane overlying the acrosome enable release of the acrosomal content – proteolytic enzymes, e.g. hyaluronidase and acrosin (Yanagimachi, 1994). Loss of these anterior portions of the membrane reveals the inner acrosomal membrane, which together with the original posterior head plasma membrane forms the new head cell membrane of acrosome-reacted sperm. The newly exposed inner acrosomal membrane represents a further source of molecules that could be involved in digestion of a pathway for the sperm through the zona or in sperm-egg fusion.

Where spermatozoa are when they acrosome react and what signal(s) causes them to acrosome react are not completely clear. Binding of the sperm to the zona pellucida (ZP), an extracellular glycoprotein coat surrounding the oocyte, can induce the acrosome reaction, but molecules that sperm contact earlier in their progress through the female reproductive tract may also facilitate or induce the acrosome reaction. These include molecules in oviductal and follicular fluids (e.g. progesterone) and also components of surrounding cells and matrix. It is possible that subpopulations of sperm acrosome react at different sites on their passage to the egg.

To reach the zona spermatozoa first have to penetrate the substantial cumulus cell barrier surrounding ovulated eggs of most mammalian species. For this purpose sperm use hyperactivated motility (Yanagimachi, 1994) and a glycosylphosphatidylinositol (GPI)-anchored surface hyaluronidase, named PH-20 (Lin et al., 1994). Hyperactivation and surface hyaluronidase are necessary, and perhaps sufficient, to digest a path through the extracellular matrix of the cumulus cells. No proteases involved in this process have been identified so far.

When spermatozoa reach the zona pellucida they recognize it and bind to it. Although there is no strict species specificity in terms of which sperm will bind to a particular zona pellucida, there is often a strong preference for binding between sperm and zona of the same species (Rankin et al., 1998). In mouse, the zona pellucida is composed of three glycoproteins called ZP1, ZP2 and ZP3. Numerous studies have indicated that acrosome-intact mouse sperm initially bind to the carbohydrate region of ZP3 (Primakoff and Myles, 2002).

The identity of the ZP3 partner molecule on the sperm surface remains elusive. Although many candidates (≈15) have been proposed, none of them has found wide acceptance. The methods used so far to establish that a candidate has a required function in sperm adhesion to the zona have not been definitive. An attempt to confirm sperm-zona adhesion activity by gene knock-out has been reported for only one sperm protein that putatively binds ZP3, a sperm surface enzyme, galactosyl transferase (GalT). GalT binds to one of its substrates (N-acetylglucosamine) on the zona and, because the second substrate (UDP galactose) is missing, sperm remain bound (Primakoff and Myles, 2002).

If sperm are acrosome-intact when they bind to the zona, they are induced to undergo the acrosome reaction as a result of binding. The acrosome reaction has been induced experimentally by the clustering of sperm surface molecules using the multivalent zona protein ZP3, or using antibodies that recognize specific sperm membrane molecules. ZP3-induced exocytosis of the acrosomal contents proceeds through two sperm signaling pathways. In the first, ZP3 binding to GalT and other potential receptors results in activation of a heterotrimeric GTP-binding protein and phospholipase C, thus elevating the concentration of cytoplasmic Ca^{2+}. In the second pathway ZP3 binding to the same receptor(s) stimulates a transient influx of Ca^{2+} through T-type calcium channels. In a later phase, these initial ZP3-induced events produce additional Ca^{2+} entry, as it was suggested through TRP channels, resulting in a sustained increase in cytoplasmic Ca^{2+} that triggers exocytosis (Jungnickel et al., 2001; O'Toole et al., 2000). It is also reasonable to notice that the molecular identity of Ca^{2+} channels involved at a later stage still remains elusive, although some candidates including TRPC2 were proposed.

Acrosome-reacted sperm are also able to bind to the zona pellucida. It has been shown in guinea pig that acrosome-reacted sperm can initiate binding to the zona

pellucida as effectively as acrosome-intact sperm, and this may also be true for rabbit and human sperm. In all species it is presumed that, after the acrosome reaction, the sperm must bind or rebind at least until zona penetration has begun so that they will not be lost from the zona surface. In mouse there is some evidence that the binding of acrosome-reacted sperm occurs to ZP2. The identity of the binding partner(s) on acrosome reacted sperm is still being researched.

In order for sperm to reach the egg plasma membrane they must penetrate through the zona pellucida. This may involve digestion of a path through the zona and could require enzymes either released by acrosome reacting sperm, or associated with the sperm surface, including the newly inserted inner acrosomal membrane. Only acrosome-reacted sperm have been observed to penetrate through the zona. Motility is maintained during penetration and the narrow penetration slit in the zona that the sperm move through may also be created, in part, by mechanical forces.

1.1.6. Sperm-egg fusion

When sperm penetrate the zona they come to lie in the narrow space between the inner boundary of the zona and the egg plasma membrane, the perivitelline space. At this stage the sperm will first bind to the egg plasma membrane and then fuse with it. There may be more than one mechanism that allows sperm to bind, because sperm from heterologous species or acrosome-intact sperm can bind without being able to fuse. The binding that is required for fusion may involve a sperm membrane protein called fertilin which probably has an egg membrane integrin as an adhesion partner. If this binding step is blocked, then fusion is also blocked. One region of the fertilin that may participate in the fusion of the two lipid bilayers contains a sequence that resembles the fusion peptide of viral fusion proteins (Chen and Sampson, 1999; Yuan et al., 1997).

Fusion results in confluency between the sperm and egg membranes as well as the sperm and egg cytoplasms. At the time of fertilization, the egg receives an unknown signal that results in a rise in intracellular free Ca^{2+} and thereby activates the egg to initiate development of the new embryo. One of the consequences of activation is completion of meiosis, including production of the second polar body, and the initiation of mitotic divisions.

1.2. Polycystic kidney disease gene family

Polycystins form an expanding gene family composed of multiple members and orthologs in fish, invertebrates, mammals, and humans that are wildly expressed in various cell types and whose biological functions remain poorly defined. The name of the family comes from autosomal dominant polycystic kidney disease (ADPKD), an inherited disorder affecting an estimated 1 in 400 to 1 in 1000 individuals of the world-wide population. ADPKD is the most common cause of renal failure in humans that is characterized by the progressive development of fluid-filled cysts in kidney and accompanied by a number of external manifestations including hepatic and brain cysts, cardiac valvular abnormalities, cerebral and aortic aneurysms, colonic diverticulae, and inguinal hernia. Genetic lesions associated with > 85% of ADPKD cases map to the PKD1 gene, > 10% are due to mutations in PKD2, and in some rare cases the third undeclared locus is involved.

Nowadays the mammalian PKD family consists of eight members that can be divided structurally into PKD1- and PKD2-like groups. Proteins similar to PKD1 (PKD1L1, PKD1L2, PKD1L3, PKDREJ) have 11 transmembrane domains and large N-terminally orientated extracellular. They are believed to function as cell surface receptors but their agonists and downstream signal transduction pathways are unknown. PKD2-like proteins (PKD2L1, PKD2L2) have 6 transmembrane domains and a pore region similar to that in Na^+, K^+ Ca^{2+} and transient receptor potential (TRP) channels. As it has been demonstrated, PKD2 and PKD2L1 act as Ca^{2+} permeable cation channels but no functional data concerning PKD2L2 are available.

Interestingly, interaction between members of different PKD subfamilies was noticed. Thus, PKD1 interacts with PKD2 and is required for the PKD2 (and PKD2L1) plasma membrane trafficking. New evidence indicates that PKD1 and PKD2 form functionally associated subunits of a receptor–ion channel complex in which PKD1 acts as a receptor that gates Ca^{2+}-permeant PKD2 channel. This polycystin complex has been found in the primary cilia of renal epithelial cells and may be involved in the transduction of Ca^{2+}-dependent mechanosensitive signal in response to cilia bending (Delmas, 2004).

1.2.1. Polycystins in male reproduction

So far, nothing is known about polycystins function in mammalian reproductive tissues and in sperm in particular, although expression of all PKD family members can be detected in testis (Fig. 1.2.).

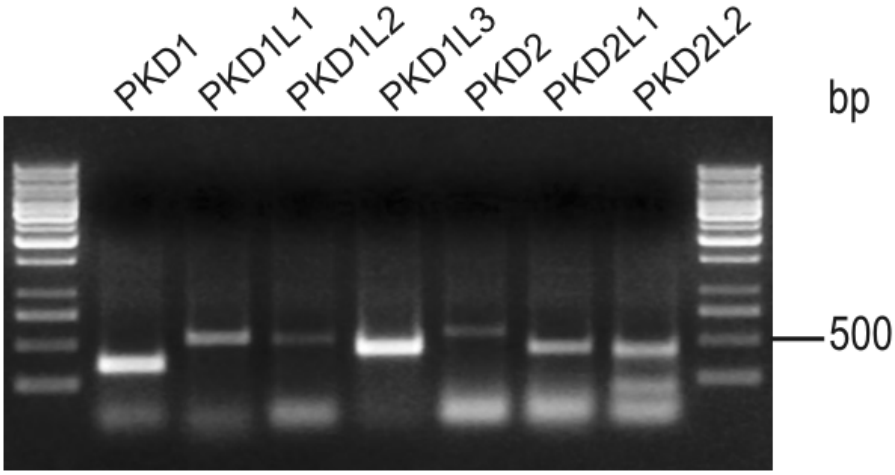

Figure 1.2. Diagnostic RT-PCR for PKD gene family members mRNA expression in mouse testis

Total RNA was isolated from mouse testis and subjected to RT-PCR with specific to each gene primer pair.

Current hypotheses on their functional relevance for reproduction are derived from knock-out models in worms and flies. Thus, the *Caenorhabditis elegans* homologues of PKD1 and PKD2, lov-1 and pkd-2, were shown to participate in male mating behavior (Barr and Sternberg, 1999; Kaletta et al., 2003). Male worms are presumed to find hermaphrodites and locate the vulva via chemical cues and sense contact with the sensory rays in the male tail. While wild-type *C. elegance* males are attracted to hermaphrodites and rapidly locate the vulva, males deficient in either or both lov-1 and pkd-2 are dramatically less successful in locating the vulva, resulting in significantly decreased male mating efficiencies.

Recently it was also demonstrated that the PKD2 homologue of *Drosophila melanogaster* is required for male fertility (Gao et al., 2003; Watnick et al., 2003). This protein is localized to the distal tip of sperm flagella and is specifically expressed in the male germline. A targeted mutation of the gene causes almost complete sterility without affecting spermatogenesis. Both the structure of the testis and the characteristics of sperm motility in the pkd-2 mutant and the wild-type fly are normal. However, sperm of

the mutant deposited in the uterus is unable to enter the female sperm storage organs (seminal receptacles and spermathecae), thus suggesting a sperm storage defect.

1.2.2. Sea urchin receptor for egg jelly proteins

In the sea urchin sperm the AR is triggered by glycoproteins in the egg jelly that can be considered to function as mammalian ZP proteins. Unlike mammalian sperm ZP3 receptor the sea urchin receptor for egg jelly (suREJ) was identified in 1996 (Moy et al., 1996). It is a 210 kDa sperm membrane glycoprotein composed from several structural domains including receptor for egg jelly domain (REJ), which shares extensive homology with mammalian PKD1-like proteins. suREJ has one putative transmembrane domain at the extreme C-terminus, with only 15 residues being cytoplasmic and is localized on the sperm plasma membrane over the acrosomal vesicle. Monoclonal antibodies against REJ domain cause Ca^{2+} influx into sperm inducing the AR and purified suREJ absorbs the AR-inducing activity of the egg jelly. The protein described above is now called suREJ1, since suREJ2 and suREJ3 proteins were recently identified, and the sequence of suREJ4 protein can be found in the database (Mengerink et al., 2000).

The suREJ2 protein is quite different from suREJ1. It consists of about 1500 amino acids, has 2 transmembrane domains and is present in the entire sperm plasma membrane concentrating over the sperm mitochondrion (Galindo et al., 2004). Experimental evidence suggests that suREJ2 does not project extracellularly from the plasma membrane but is an intracellular plasma membrane protein. The possible function of suREJ2 is anchoring the mitochondrion to the plasma membrane and maintaining its position as the sperm cytoplasm shrinks and the nucleus becomes triangular.

The third suREJ3 protein is the closest homolog to mammalian PKD1-like proteins. It contains about 2700 amino acid residues, has 11 putative transmembrane segments and last 6 of them are homologous to voltage-dependent Ca^{2+} cannels. Despite all three suREJ proteins possess GPS domain, in fact only suREJ3 is post-translationally cleaved and the both halves of the protein remain associated co-localizing exclusively to the acrosomal vesicle region of the sperm (Mengerink et al., 2002). Recently, it was reported that sea urchin PKD2 homolog associates with suREJ3 in the plasma membrane over the sperm acrosomal vesicle but it is still unclear, whether both proteins

interact directly or through any other scaffolding protein (Neill et al., 2004). While the role of suREJ1 in AR is determined as a sperm receptor for the egg glycoprotein coat, participation of the suREJ3 protein in AR signaling remains pure speculation. Although some data suggest its possible role in sea urchin AR (Neill and Vacquier, 2004), further studies have to be done to understand the real function of suREJ3 in spermatozoa.

1.2.3. Polycystic kidney disease and receptor for egg jelly

Both human and murine PKDREJ genes were identified in 1999 by Hughes et al. The mouse gene encoding PKDREJ consists of only one exon located on chromosome 15 with an open reading frame (ORF) of 6381 base pairs (bp). The translated protein is 2126 amino acids long and shows about 35 % similarity to both PKD1 and PKD2.

Hydrophobicity plot analysis of the PKDREJ sequence predicts a membrane protein with 11 transmembrane regions (Fig. 1.3.). Also several functional domains can be identified in PKDREJ including a cleavable signal peptide, a receptor for egg jelly (REJ) module, a G-protein-coupled receptor (GPCR) proteolytic site domain (GPS), a PLAT/LH (Polycystin-1, Lipoxygenase, Alpha-Toxin / Lipoxygenase homology) domain and an ion channel region.

Receptor for egg jelly domain. The REJ domain is 600 amino acids long, so it is probably composed of multiple structural domains. It has six completely conserved cysteine residues that may form disulphide bridges. The domain is found also in PKD1, and the sea urchin sperm receptor for egg jelly proteins. The function of this domain is unknown.

G-protein-coupled receptor proteolytic site domain. This domain has been originally discovered in latrophilin, and later was found in many otherwise unrelated cell surface receptors. Proteolytic cleavage within the GPS domain has been shown for latrophilin and some other GPCRs, but it also occurs in PKD1 and sea urchin REJ3 – the closest PKDREJ homolog among suREJ proteins. In PKDREJ the GPS domain is about 70 amino acids long, whereas in other proteins it has no more that 55 residues. Multiple sequence alignment of GPS domains of proteins already shown to be cleft with that of PKDREJ elicited some distinctions of principle. The highly conserved cleavage motif H L ^ T (where " ^ " indicates the position of cleavage) in both human and mouse PKDREJ contains an additional histidine residue and is present as H L H T. Moreover, in PKDREJ two conserved cysteine residues are absent directly before the cleavage

motif and can be found only in 20 amino acids N-terminal to the predicted cleavage site. Recently, it was shown that cleavage in GPS domain is an autocatalytic intramolecular reaction, which does not require any proteases involvement (Lin et al., 2004).

Polycystin-1, Lipoxygenase, Alpha-Toxin / Lipoxygenase homology domain. The PLAT/LH domain is found in a variety of membrane or lipid associated proteins. It is present at the N-terminus of lipoxygenases, enzymes involved at various steps in the biosynthesis of leukotrienes with iron as a cofactor, and at the C terminus of lipases. Both types of enzymes are cytosolic but need this domain to access their sequestered membrane or micelle bound substrates. The known structure of pancreatic lipase shows this domain binds to procolipase that mediates membrane association. This domain may

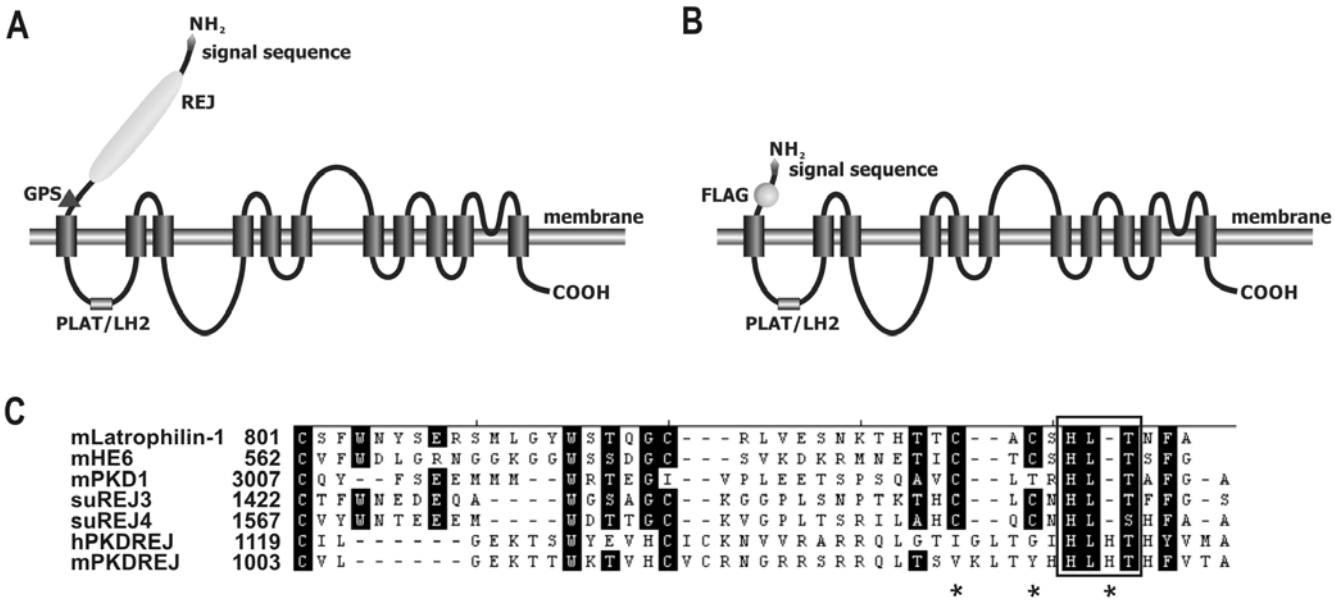

Figure 1.3. Schematic diagram of PKDREJ domain organisation

Predicted topology and domain structure of PKDREJ **(A)** and its N-terminally truncated mutant PKDREJΔ(20-1023) **(B)**. PKDREJ possess a large extracellular domain including the REJ domain, a GPS cleavage site, eleven transmembrane domains, an intracellular PLAT/LH domain between TM 1 and TM2. Note that PKDREJ shares features characteristic of a cation channel, namely 6 transmembrane domains and a pore region between the last two C-terminal transmembrane domains. REJ – Receptor for Egg Jelly domain; GPS - G-protein-coupled receptor proteolytic site domain; PLAT/LH - Polycystin-1, Lipoxygenase, Alpha-Toxin / Lipoxygenase homology domain; FLAG – 8-amino acid peptide recognized by anti-FLAG antibodies. **(C)** Multiple sequence alignment of GPS domains. The conserved cleavage motif is marked by frame. Asterisks indicate main distinctions between PKDREJ GPS domain and these of proteins shown to be cleaved.

also mediate membrane attachment via other protein binding partners. Structurally it consists of an eight stranded beta-barrel. In PKDREJ PLAT/LH domain is located between two fist transmembrane domains on the intracellular loop.

Ion channel region. Like suREJ3, but in contrast to PKD1, PKDREJ has a putative pore region similar to that in sodium, potassium and calcium ion channels. Usually these channels have 6 transmembrane helices where the last two helices flank a loop, which determines ion selectivity. In some subfamilies (e.g. Na^+ channels) the domain is repeated four times, whereas in others (e.g. K^+ channels) the pore is formed by tetramerisation of single subunits. Although the PKDREJ has 11 transmembrane domains and belongs to the PKD family, alignment of its pore sequence displays homology to mucolipins – a subfamily of transient receptor potential (TRP) channels, rather than to PKD2-like proteins.

Although the PKDREJ gene was identified in 1999, nothing is known about the protein so far. The only available data that make the gene highly interesting for reproductive biology are homology to the sea urchin REJ proteins and testis specific mRNA expression coincident with the onset of sperm maturation (Hughes et al., 1999). Having a large extracellular REJ-domain and a putative pore region PKDREJ may function as both a receptor and/or an ion channel in the chain of signaling events leading to acrosomal exocytosis.

2. OBJECTIVES

The mammalian polycystic kidney disease (PKD) gene family comprises eight members whose role in cell physiology is still poorly understood. Two of the founding members of the family, PKD1 and PKD2, are responsible for the majority of cases of autosomal dominant polycystic kidney disease. While PKD1 is considered to be a cell-surface receptor, PKD2 has been described both at the plasma membrane and intracellularly and functions as a cation channel. The present study focuses on polycystic kidney disease and receptor for egg jelly (PKDREJ), a protein that contains both a large receptor-like extracellular part and a putative ion channel region. Although the PKDREJ gene was identified in 1999, nothing is known about the protein so far.

The aim of the present work is characterization of the PKDREJ gene and protein in both heterologous and native systems. PKDREJ expression, subcellular localization, tissue distribution and biochemical features are to be identified.

The homology of PKDREJ to the sea urchin REJ proteins, which participate in the sea urchin sperm-egg binding and the induction of the acrosome reaction, and testis-specific mRNA expression coincident with the onset of sperm maturation provide a hypothesis about similar task of PKDREJ in mammalian fertilization. The project is intended to investigate the role of PKDREJ in male reproduction.

3. MATERIALS AND METHODS

3.1. Materials

3.1.1. Chemicals and reagents

Name	Supplier
10mM dNTP Mix	Fermentas
2-propanol	Merck
30% acrylamide/0.8% bisacrylamide	Carl Roth
Acetone	J.T.Baker
Agarose, Electrophoreses Grade	Peqlab
BacterioMatch™ Two-Hybrid System XR Plasmid cDNA Library	Stratagene
Bacto™ agar	BD & Co
Bacto™ tryptone	BD & Co
Bacto™ yeast extract	BD & Co
Coomassie Blue G250	Carl Roth
DakoCytomation Fluorescent Mounting Medium	Dako
Deoxyribonuclease I (RNase free) supplied with 10x reaction buffer and 25mM EDTA	Fermentas
DTT	Fluka
ECL reagent	Amersham Bioscience
Ethanol	Carl Roth
Ethidium bromide	Carl Roth
Fura-2/AM	Fluka
IPTG	Fluka
METAFECTENE™	Biontex Laboratories
Methanol	Merck
NP-40	Calbiochem
Nucleofector™ Solution V	Amaxa
Plasmid DNA Purification Kit Nucleobond® AX	Macherey-Nagel

Ponasterone A	Invitrogen
Propidium iodide solution	Fluka
QIAEX® II Gel Extraction Kit	Qiagen
Restriction enzymes: AatII, ClaI	New England Biolabs
Restriction enzymes: AvrII, Bpu1102I, EcoRI, NotI, NsbI, XhoI	Fermentas
RevertAid™ H Minus M-MuLV Reverse Transcriptase supplied with 5x Reaction Buffer	Fermentas
Ribonuclease Inhibitor	Fermentas
SDS	Carl Roth
T4 ligase supplied with 10x reaction buffer	Fermentas
TEMED	Carl Roth
Tissue-Tek®	Sakura
TOPO-TA Expression Kit	Invitrogen
Tris-base	Carl Roth
TRIZOL	Gibco BLR
Tween® 20	Carl Roth
XL QuickChange Mutagenesis kit	Stratagene

All other reagents were purchased from Sigma.

3.1.2. Equipment and devices

Name	**Supplier**
Adjustable air-displacement pipettes Pipetman®	Gilson
Autoclave Varioklav®	H+P Labortechnik
Cell electroporator Nucleofector™	Amaxa
Centrifuge 5417R	Eppendorf
Centrifuge Biofuge	Heraeus
Centrifuge Megafuge 1.0 R	Heraeus
Centrifuge Sorvall RC 5B	Du Pont
CO_2-incubator Hera Cell	Heraeus
Digital Camera Digital Science DC 120 Zoom	Kodak
Expositionchamber Hypercassette™	Amersham Pharmacia

Incubatior Function Line	Heraeus
Laminar flow hood Hera Safe	Heraeus
Light microscope Wilovert A	Hund
Magnetmixer Variomag®	H+P Labortechnik
Orbital Shaker	Forma Scientific
PCR machine T3 Termocycler	Biometra
pH-measurer	Radiometer
Powersupply PowerPac 300	Bio-Rad
PVDF membrane	Amersham Bioscience
RC-5 Superspeed Refrigerated Centrifuge	Sorvall
Refrigerator -86C Freezer	Forma Scientific
Rocker Rocky® 3D	Froebel Labortechnik
Rotor SS-34	Sorvall
Tissue culture flasks 25 cm^2 and 75 cm^2	Sarstedt
Tissue culture plate 6-well	Sarstedt
Tubes 15 ml and 50 ml	Sarstedt
Ultracentrifuge L7-55	Beckman
UV-Bank UV Transilluminator 2000	Bio-Rad
UV-visible spectrometer Helios Gamma	Unicam Instruments
Vortex Genie 2	Scientific Industries
Zeiss LSM 510 META confocal laser scanning microscope	Carl Zeiss
Zeiss-EM 10C 902 electron microscope	Carl Zeiss

3.1.3. Oligonucleotides and primers

All oligonucleotides and primers were purchased from Metabion GmbH (Martinsried, Germany).

Name	**Sequence**
RT-PCR_1_f	5´-GCAGGGGTTGACGATGACACAGGA-3´
RT-PCR_1_r	5´-CTCACAAGCGGAAGGCCAAGGATT-3´
RT-PCR_2_f	5´-GGGCCAGACCTAGCAACAAGAC-3´
RT-PCR_2_r	5´-AAGAATGGCGGCGTAGAGGTAGAT-3´

RT-PCR_beg_f	5′-GGCTGCCGGGCGTGCTCA-3′
RT-PCR_beg_r	5′-CCTTCAGGGGGCGTTTTCT-3′
RT-PCR_actin_f	5′-GGCTACAGCTTCACCACCAC-3′
RT-PCR_actin_r	5′-GAGTACTTGCGCTCAGGAGG-3′
sPJ-PCR_f	5′-GAATTCGACTACAAGGATGACGACGATAAGCGGAGC CGGCGGCAGCTGA-3′
sPJ-PCR_r	5′-TCAGACAACAAGGTAAATCATTTTCTTC-3′
sPJ-EcoRI_f	5′-CTAGGCAGCCAGCGGGAATTCACCGGCCCTCGCGG-3′
sPJ-EcoRI_r	5′-CCGCGAGGGCCGGTGAATTCCGGCTGGCTGCCTAG-3′
GST-N-term_f	5′-CCTCCTGAAAGTGAATTCTTCGGACCCC-3′
GST-N-term_r	5′-CCTGCGGCTCGAGCACAGGTCGGTT-3′
GST-Loop_f	5′-GTGATGAATTCGGGAGATATCTACACCT-3′
GST-Loop_r	5′-CCCATCTTTTCCCTCGAGGCTTATAAGT-3′
GST-C-term_f	5′-GCCTAGAATTCGATGAAGCAGCCTG -3′
GST-C-term_r	5′-GTGATCTCTCGAGAACAAGGTAAATC -3′
GPSmut_f	5′-GAAGCTGACCTACCATCGTCTGCACACCCACTTTG-3′
GPSmut_r	5′-CAAAGTGGGTGTGCAGACGATGGTAGGTCAGCTTC-3′
pIND-ClaI_f	5′-GAAGAACTCACACACAGCTATCGATTAAACTTAAGC TTGGTACCG-3′
pIND-ClaI_r	5′-CGGTACCAAGCTTAAGTTTAATCGATAGCTGTGTGT GAGTTCTTC-3′
ClaI_f	5′-CCATCGATGGCTAGTTAAGCTTGGTACCGA-3′
AatII_r	5′-GGGACGTCTAGACTCGAGCGGCCGCCACTGT-3′
ClaI_mut_f	5′-GGCTAGTTAAGCTTGGTATCGATCTCGGATC CACTAGTCC-3′
ClaI_mut_r	5′-GGACTAGTGGATCCGAGATCGATACCAAGCT TAACTAGCC-3′

3.1.4. Antibodies

Name	**Host**	**Supplier**
Alexa Fluor® 488, anti-rabbit IgG	Goat	Molecular Probes

Alexa Fluor® 546, anti-rabbit IgG	Goat	Molecular Probes
Monoclonal Anti-Tubulin, acetylated	Mouse	Sigma
Anti-mouse IgG, FITC conjugate	Goat	Sigma
Polyclonal Anti-Green Fluorescent Protein	Rabbit	BD Bioscience
Anti-rabbit IgG, horseradish peroxidase conjugate	Goat	Amersham Bioscience
EM anti-rabbit IgG, 10 nm gold conjugate	Goat	BBInternational
Anti-GST, horseradish peroxidase conjugate	Rabbit	Amersham Bioscience

3.1.5. Cell culture supplements

Name	**Supplier**
DMEM high glucose with L-Glutamin	PAA
Fetal calf serum (FCS)	PAA
Hygromycin B	PAA
Penicillin/Streptomycin	PAA
Phosphate-buffered saline (PBS)	PAA
Trypsin/EDTA	PAA
Zeocin	Invitrogen

3.1.6. Immortalized cell lines

Cell line	**Characteristic**	**Source**
HEK293	Adherent	Human embryonic kidney
COS7	Adherent	Simian fibroblasts
GC-1	Adherent	Murine spermatogonia type B
GC-2	Adherent	Murine early spermatids
EcR-293	Adherent	HEK293 cells stably expressing the ecdysone receptor and the retinoid X receptor
EcR-P4	Adherent	EcR-293 cells inducibly expressing mouse PKDREJ

3.1.7. Buffers and standard solutions

10x PBS (Phosphate-buffered saline)

NaCl	1.5 M
Na_2HPO_4	52 mM
KH_2PO_4	17 mM

PBS-T

NaCl	150 mM
Na_2HPO_4	5.2 mM
KH_2PO_4	1.7 mM
Tween 20	0.05% (v/v)

50x TAE (Tris/acetate/EDTA) electrophoresis buffer

Tris base	2 M
Glacial acetic acid	1 M
EDTA (pH 8.0)	0.05 M

5x SDS electrophoresis buffer

Tris base	125 mM
Glycine	960 mM
SDS	0.5 % (w/v)

Electrophoresis transfer buffer

Tris base	50 mM
Glycine	380 mM
SDS	0.1 % (w/v)
Methanol	20 % (v/v)

LB medium

Tryptone	1 % (w/v)
Yeast extract	0.5 % (w/v)
NaCl	170 mM

LB-agar

Tryptone	1 % (w/v)
Yeast extract	0.5 % (w/v)
NaCl	170 mM
Agar	2 % (w/v)

S1 resuspension buffer

Tris-HCl (pH 8.0)	50 mM
EDTA	10 mM
RNase A	100 µg/ml

S2 lysis buffer

NaOH	200 mM
SDS	1 % (w/v)

S3 neutralization buffer

KAc (pH 5.1)	2.8 M

Modified RIPA buffer

Tris-base (pH 7.5)	20 mM
NaCl	150 mM
EDTA	1 mM
Sodium deoxycholate	0.5 % (w/v)
NP-40	1 % (v/v)
SDS	0.1 % (w/v)

1 tablet “Complete Mini” protease inhibitor cocktail to 7 ml of volume

Recipes of buffers used for single experiment are given further in methods descriptions.

3.2. Methods

3.2.1. General laboratory techniques

3.2.1.1. Sterilization of solutions and work materials

Solutions, tubes, glassware, plastics, deionized H_2O and other items were sterilized by autoclaving for 20 min at 121°C.

3.2.1.2. Plasmid DNA purification

Mini plasmid DNA preparation was performed as following. Bacteria were collected in 2 ml eppendorf tubes, centrifuged for 2 min at the maximal speed, supernatant was carefully aspirated and the bacterial pellet was extensively resuspended in 150 µl S1 biffer. Then the equivalent amount of S2 lysis buffer was added, suspension was carefully shacked and incubated at room temperature for 2 min prior to neutralisation with 150 µl S3 buffer. After centrifugation for 20 min at maximal speed the supernatant was collected in a fresh 1.5 ml eppendorf tube, 950 µl of 100% ethanol were added and DNA was precipitated by centrifugation for 20 min. The DNA pellet was then washed with 1 ml of 70% ethanol and let air-dry for about 10 min before dissolved in $_{dd}H_2O$.

Midi DNA preparations were performed using Plasmid DNA Purification Kit Nucleobond® AX (Macherey-Nagel) according manufacturer instructions.

3.2.1.3. Determination of DNA and RNA concentrations

A spectrophotometer was used to measure the concentration of nucleic acids in solutions. 2µl of DNA or RNA samples were added to 98 µl sterile H_2O (1:50 dilution) for an optical density (OD_{260nm}) reading. The DNA concentration was determined based on the fact that an absorption of 1 at 260nm is equivalent to a DNA concentration of 50µg/ml. Absorption (OD_{260nm}) × 50 µg/ml × Dilution Factor (50) = µg/ml DNA. For RNA, an absorption of 1 at 260nm corresponds to an RNA concentration of 40 µg/ml. Absorption (OD_{260nm}) × 40 µg/ml × Dilution Factor (50) = µg/ml RNA. The purity of nucleic acid in solution can be determined by dividing the absorption's ($OD_{260/280nm}$), as peptides bonds absorb UV light at 280nm. Protein contaminated DNA or RNA solutions have a ratio of < 1.7.

3.2.1.4. Work with RNA

Precautions were used while isolating and handling RNA in order to prevent degradation. All used solutions, glassware and plastics were sterilized to ensure the absence of RNase, which is an extremely stable enzyme requiring no cofactors to exert its effect of RNA digestion and degradation. Everything was handled only while wearing gloves. RNA was always dissolved in DEPC-H_2O and stored at –80°C or on ice while handling.

3.2.1.5. Work with DNA

Although DNA is by far not as sensitive to degradation as RNA it was also kept on ice while working with it and stored in a freezer at –20°C.

3.2.1.6. DNA agarose gel electrophoresis

Usually 1% (w/v) agarose was added to 100ml 1 × TAE buffer and heated until the agarose was completely dissolved. Next, 5µg/ml ethidium bromide was added to the gel solution for DNA visualisation and the gel was poured into a gel tray. Before its polymerization (20 min.) combs were placed in the gel to create wells. The DNA solutions (i.e. plasmid DNA or PCR product) were mixed with DNA loading buffer (5:1) and loaded in the wells. The DNA fragments were separated by electrophoresis in parallel to a 1 kb DNA ladder at 60-80 volts in 1 × TAE buffer. DNA bands were detected under UV light or on an UV bank.

3.2.1.7. Work with immortalized cell lines

Handling of immortalized cell lines

Handling and propagation of all cell lines were performed in a cell and tissue culture laminar-flow hood under sterile conditions. All solutions were stored at 4°C and warmed up to 37°C in a water-bath before using. All solutions were only opened under sterile conditions in a hood. Cell culture media, FCS and other supplements used for all cell lines are indicated in Table 3.1.

Table 3.1. Culture media and supplements used for maintenance of immortalized cell lines

Cell line	Complete Medium	Supplements	Freezing Medium
HEK293	DMEM (high glucose) 10% fetal calf serum 1% Pen-Strep	—	90% complete medium 10% DMSO
COS7	as above	—	as above
GC-1	as above	—	as above
GC-2	as above	—	as above
EcR-293	as above	400 µg/ml Zeocin	as above
EcR-P4	as above	400 µg/ml Zeocin 400 µg/ml Hygromycin	as above

Thawing of immortalized cell lines

The cell line aliquots were stored in 1 ml freezing medium at liquid nitrogen. To grow up a cell line the freeze down was thawed quickly in a 37°C water-bath then transferred into a cell culture flask where mixed with at least 10 ml of antibiotic-free medium. After 1 hour recovery the medium was replaced with the one containing antibiotics and all other usual supplements. The cells were grown further in a 5% CO2, 37°C incubator.

Maintenance of immortalized cell lines

All cell lines were grown in a humidified atmosphere of 5% CO2 / 95% air at 37°C. Cells were split in certain ratios depending on the stage of confluence and the proliferation rate of each cell line. The amount of medium added to the flask was dependent on its size. 10 ml were added into 75 cm2 flasks whereas 5 ml were added to the 25 cm2 flasks. 1/10 of the amount of culture medium was used as the amount of Trypsin/EDTA supplied to a culture flask in order to detach the cells. To split cells the medium was completely aspirated from the flask and the cells were washed briefly with 10 ml of PBS to remove traces of antitrypsin originating from the serum in the media. After removing the PBS 5 ml Trypsin/EDTA were placed into the 75 cm2 and 2 ml into the 25 cm2 flasks. Cells detached after about 2 min with occasional gentle tapping. The Trypsin/EDTA was then immediately inactivated by adding equivalent amount of

medium to each flask, the cell suspension was pipette up and down 10 times and the appropriate amount was split into a new flask.

Freezing cultured immortalized cell lines

To freeze cells for long term storage, cells were harvested (at least one T75 flask of 80 % confluent cells) and centrifuged at 1,000 g for 5 minutes. The media was then aspirated and cells were resuspended in 1 ml of cell culture freezing medium (Table 3.1.). The resuspended cell solution was transferred to criovial and placed at –80°C in an isopropanol-containing cell freezing container, which guarantees a slow freezing process. After 24 hours the vial was placed in a regular box and transferred into liquid nitrogen.

3.2.2. Cell culture and cell biology methods

3.2.2.1. Transfection of HEK293, COS7 and EcR293 cells

Transient transfection of HEK293, COS7 and EcR293 cells was carried out using METAFECTENE™ transfection reagent. Prior to transfection, cells were grown until 80% confluent in 6-well plates in 1.5 ml of medium per well. For one well 1.5 – 2.5 µg DNA and DNA / METAFECTENE™ ration 1:3 (w/v) were used. DNA and METAFECTENE™ were separately dissolved in 50 µl DMEM medium free of serum and antibiotics, then mixed together in one tube, incubated at room temperature for 30 min and finally added to the cells. Cells were incubated with the DNA / METAFECTENE™ mixture for 24 hours before further use.

3.2.2.2. Electroporation of GC-1 and GC-2 cells

Electroporation of GC-1 and GC-2 cells was performed using Nucleofector™ device, Nucleofector™ Solution V and the programme T-27 according to the manufacturer's instructions without any modifications.

3.2.2.3. Generation of PKDREJ inducible cell lines (EcR-P4)

For generation of EcR-P4 cell line mouse PKDREJ cDNA was subcloned into pIND(SP1)/Hygro expression vector (3.2.3.10.) and linearized with NsbI restriction enzyme at 37°C overnight. Next day the enzyme was inactivated by heating at 65°C for

20 min, DNA was precipitated and subsequently diluted in the same amount of water as it was before the restriction. EcR-293 cells grown in eight 11-mm dishes were transfected using METAFECTENE™ transfection reagent (3.2.2.1.) and allowed to recover for 1 day prior to the selection with hygromycin (400 µg/ml). After 14 days of the selection 26 positive clones were picked each into a separate well of 12-well plate and propagated for the next two weeks to reach amount about 10^6 cells sufficient for detection of PKDREJ expression by RT-PCR.

3.2.2.4. Induction of PKDREJ expression in EcR-P4 cell lines with ponasterone A

Ponasterone A was prepared as a 1mM stock solution in 100 % ethanol. Prior to induction, EcR-P4 cells were grown until 80 % confluent. For the induction of the PKDREJ expression an old medium in a culture flask was completely replaced a with fresh medium containing the appropriate ponasterone A concentration. Normally ponasterone A was used in the final concentration of 5 µM and the cells were incubated with the drug for 20 hours.

3.2.2.5. Primary culture of mouse aortic smooth muscle cells

Mouse aortic SMC were obtained from 6-12 week old mice of both gender. Normally four to six mice were used for each experiment. Mice were killed by cervical dislocation, aortas were cut out, and rinsed several times in the ice-cold isolation buffer. After adventitia and surrounding tissues were removed, aortas were cut longitudinal, minced to smaller pieces, placed into 1 ml digestion mix I and incubated for 30 min in the water bath at 37°C with a gentle agitation. The suspension then was centrifuged at 200 g for 10 min, the pellet was carefully resuspended in 1 ml digestion mix II and incubated 10 min more in the same water bath. After following centrifugation the cellular digest was resuspended once again in 1 ml isolation buffer, pushed through a self-made glass pipette for final cell dissociation and placed onto the poly-L-lysine coated glass cover slips in SmGM®-2 (Cambrex, Verviers, Belgium) medium. Cells were cultured for five to seven days before used for immunocytochemical experiments.

Isolation Buffer

NaCl	127 mM
KCl	5,9 mM
$MgCl_2$	1,2 mM
Glucose	11,8 mM
HEPES (pH 7.4)	10 mM

Digestion Mix I (prepared in isolation buffer)

Albumin	1 mg/ml
Papain	0,7 mg/ml
DTT	1 mg/ml

Digestion Mix II (prepared in isolation buffer)

Albumin	1 mg/ml
Collagenase H	1 mg/ml
Hyaluronidase	1 mg/ml
$CaCl_2$	0,05 mM

3.2.2.6. Mouse sperm isolation

For mouse sperm isolation 6-12 weeks male mice were used. Animals were killed by cervical dislocation and the caudae epididymidis and vasa deferentia were excised and cleaned in HS buffer or PBS. The tissue than was transferred to 1 ml HS buffer, incised 5–10 times with a scissors and incubated for 15 min at 37°C and 5% CO2 to allow sperm to exude into the buffer. Afterwards sperm were collected, washed twice by diluting to 2 ml and centrifuging (500 g, 5 min). The final concentration for further use was 1–2 x 10^7 cells/ml.

HS buffer

NaCl	135 mM
KCl	5 mM
$MgSO_4$	1 mM
$CaCl_2$	2 mM

HEPES (pH 7.4)	3 mM
Glucose	10 mM
Lactic acid	10 mM
Pyruvic acid	1 mM

3.2.2.7. Preparation of unfractionated zona pellucida glycoproteins

Unfractionated ZP glycoproteins were prepared as previously published (Jungnickel et al., 2001). Ovaries from 20 female mice were homogenized in 2 ml HB complete medium and the homogenate was fractionated on a 3-step percoll gradient (22/10/2 %). After 2 hours of centrifugation at 200 g and 4 °C, the ZP-containing 10%-percoll fraction was collected, diluted with HB complete medium to 15 ml and ZPs were subsequently concentrated by several centrifugation steps at 16000 g at 4 °C. Soluble ZP glycoproteins were prepared by a two-step extraction for 20 min each with 5 mM sodium phosphate (pH 2.5) at 60 °C. Thereafter, insoluble material was removed by centrifugation at 16000 g for 1 min and the supernatant was used immediately for the induction of the AR at a final concentration of 5 ZP/µl.

HM complete medium (pH 8.5)

NaCl	150 mM
$MgCl_2$	1 mM
$CaCl_2$	1 mM
Triethanolamin	25 mM
Aprotinin	0.2 mg/ml
DNase	0.2 mg/ml
Nonidet NP-40	1% (v/v)
Sodium deoxycholate	1% (w/v)

1 tablet “Complete Mini” protease inhibitor cocktail to 50 ml of volume

3.2.2.8. Mouse sperm capacitation and induction of the acrosome reaction

Isolated mouse caudae epididymides and vasa deferentia were rinsed in 37°C warm PBS, the fat tissue and blood vessels were cut out, the organs were placed into 1 ml of warm WH medium, incised 5–10 times with a scissors and incubated for 10 min at 37°C and 5% CO2 to allow sperm to exude into the buffer. The medium with sperm

was collected, diluted with WH medium to 10 ml and centrifuged (500 x g, 10 min). Afterwards the sperm was resuspended in 1 ml of the buffer and incubated additionally 60 min at 37°C and 5% CO2 for sperm capacitation. When antibodies were used, 6 µg/ml of them were added to the sperm suspension 30 min before induction of AR to allow antibody binding. After AR-inducers were added the cell suspension was additionally incubated 30 min at 37°C and 5% CO2, the reaction was stopped by fixing the sperm and acrosome status was examined by Coomassie Blue staining (3.2.2.9.).

Whitten-HEPES (WH) medium

NaCl	100 mM
KCl	4.7 mM
KH_2PO_4	1.2 mM
$MgSO_4$	1.2 mM
$CaCl_2$	2 mM
HEPES (pH 7.4)	20 mM
Glucose	5.5 mM
Lactic acid	4.8 mM
Pyruvic acid	1 mM
$NaHCO_3$	20 mM
BSA	10 mg/ml

3.2.2.9. Determination of sperm acrosome reaction status

After induction of acrosome reaction (3.2.2.7) sperm suspension was fixed in 5-fold volume of fixating solution for at least 10 min. Afterwards cells were centrifuged briefly (13000 × g, 1 min), washed in 5-fold volume of ammonium acetate buffer and centrifuged again. The cell pellet was resuspended in 15 µl of ammonium acetate buffer, the suspension was spotted onto glass slides and air dried. After staining with 0.04% coomassie blue for 5 min at room temperature slides were rinsed in distillated water, air dried and mounted. The cells with a dark blue staining of the acrosome were counted as acrosome-intact whereas these with no staining of acrosomal region were considered to be acrosome reacted.

Fixating solution

Na_2HPO_4	20 mM
NaCl	150 mM
Formaldehyde	7.5 % (v/v)

Ammonium acetate buffer

Ammonium acetate, pH 9.0	100 mM

Coomassie Blue staining solution

Coomassie Blue G250	0.04 % (w/v)
Methanol	50 % (v/v)
Acetic acid	10 % (v/v)

3.2.2.10. Expression of PKDREJ proteins in *Xenopus laevis* oocytes

cDNAs of PKDREJ and its mutants were subcloned into the pOG-I vector, a pBluescript derivative with the 5´ and 3´ UTRs of Xenopus ß-globin (3.2.3.10.), and linearised overnight by SacII digestion prior to in vitro transcription. 10ng of in vitro transcribed cRNA (mMESSAGE mMACHINE kit, Ambion, Austin, TX) for each PKDREJ construct was injected into defolliculated Xenopus oocytes, which were kept in ND96 solution at 16°C. Three to five days after injection, two-electrode voltage-clamp measurements were performed with a GeneClamp 500 amplifier (Axon Instruments, Foster City, CA) at room temperature. Currents were recorded in ND96 solution without sodium pyruvate, theophylline, and gentamicin.

ND96 solution

NaCl	96 mM
KCl	2 mM
$CaCl_2$	1.8 mM
$MgCl_2$	1 mM
HEPES (pH 7.4)	5 mM
Sodium pyruvate	2.5 mM
Theophylline	0.5 mM
Gentamicin	20 µg/ml

3.2.3. Molecular biology methods

3.2.3.1. Preparation of chemically competent *Escherichia coli* cells

To prepare chemically competent *E.coli* cells DH5α strain was used. Cells were plated on an LB-agar plate and incubated overnight at 37°C. Next day a single colony approximately 2 mm in diameter was inoculated in 250 ml SOB medium and the flask was incubated at 18°C with 180 rpm shaking for 2-3 days until the cells density of 0.6 OD600nm was reached. Before harvesting the cells the flask was kept on ice for 10 min. Afterwards centrifugation at 2500 g and 4°C for 10 min was performed, the pelleted cells were resuspended in 80 ml of ice-cold transformation buffer and incubated for another 10 min on ice. Second centrifugation was carried out as described above. The pellet was then resuspended in 18.6 ml of ice-cold transformation buffer and 1.4 ml DMSO was slowly added with gentle stirring to the final concentration of 7 % (v/v). After 10 min incubation on ice cells were aliquoted in eppendorf tubes, freezed immediately in liquid nitrogen and placed at -80°C for storage.

SOB medium

Tryptone	2 % (w/v)
Yeast extract	0.5 % (w/v)
NaCl	10 mM
KCl	2.5 mM
$MgCl_2$	10 mM
$MgSO_4$	10 mM

Medium was prepared and autoclaved without magnesium. Filter sterilized stock solutions of 1 M $MgCl_2$ and 1 M $MgSO_4$ were added directly before use.

Transformation buffer

PIPES	10 mM
Yeast extract	15 mM
$CaCl_2$	10 mM
KCl	250 mM
$MnCl_2$	55 mM

The buffer was made without manganese, pH was adjusted to 6.7 and then $MnCl_2$ was added.

3.2.3.2. Transformation of chemically competent *Escherichia coli*

An eppendorf tube containing 100 µl of frozen chemically competent *E.coli* in transformation buffer (3.2.3.1.) was thawed on ice, appropriate amount of plasmid DNA (up to 10 µl) was added and the tube was kept on ice for other 30 min. After "heat shock" at 42°C for 30 seconds, the tube was placed on ice for 2 min and then the cells were spread on an LB-agar plate containing appropriate antibiotic or other selective marker. The plate was incubated at 37°C overnight until positive colonies could have been analyzed and proceeded.

3.2.3.3. Diethylpyrocarbonate (DEPC) treatment of water

200 µl of DEPC was added to 100 ml of $_{dd}H_2O$, shacked vigorously to get DEPC into solution and finally autoclaved to reactivate the remaining DEPC.

3.2.3.4. Isolation of total RNA from various mouse tissues and cultured cells

Various mouse organs were isolated, frozen in liquid nitrogen and grinded. Afterwards 50-100 mg of each tissue were homogenized in 1 ml TRIZOL® reagent by intensive pipeting, 0.2 ml of chloroform was added and the tubes were shacked vigorously by hand for about 15 seconds. Following 3 min incubation at room temperature the samples were centrifuged at 12000 g for 15 min at 4°C and containing RNA colorless upper aqueous phase was transferred in a fresh tube. After addition of 0.5 ml of isopropanol samples were incubated for 10 min at room temperature, RNA was precipitated by centrifugation at 12000 g for 10 min at 4°C and the pellet was washed once in 1 ml of 75% ethanol. Following the centrifugation at 7500 g for 5 min at 4°C supernatant was discarded, the RNA pellet was briefly dried and dissolved in RNAse-free DEPC-treated water by passing the solution a few times through a pipette tip and incubation for 20 min at 60°C.

For RNA isolation from cultured cells GeneElute™ Mammalian Total RNA Miniprep Kit purchased from Sigma was used and the procedure was performed according the protocol of the manufacturer.

3.2.3.5. Preparation of DNA-free RNA prior to RT-PCR

To dispose of probable genomic DNA contamination DNase I treatment of isolated total RNA was performed. To an RNase-free tube were added 1 µg of RNA, 1 µl of 10× reaction buffer with MgCl2, DEPC-treated water to 9 µl and 1 µl of deoxyribonuclease I (1 u/µl). After 30 min incubation at 37°C 1 µl of 25 mM EDTA was added and the tube was heated at 65°C for 10 min to inactivate deoxyribonuclease I. From the final mixture 1 µl was taken out for PCR as a control of complete DNase I treatment and the rest 10 µl of prepared DNA-free RNA was directly used as a template for reverse transcriptase.

3.2.3.6. First strand cDNA synthesis

10 µl containing approximately 1 µg of DNA-free RNA was used as a template for the first strand cDNA synthesis. The procedure employed random hexamer primer and RevertAid™ H Minus M-MuLV Reverse Transcriptase purchased from Fermentas and was performed according the protocol of the manufacturer without any modifications. The synthesized cDNA was directly used for PCR amplification.

3.2.3.7. RT-PCR for detection of PKDREJ mRNA

For detection of mPKDREJ expression by RT-PCR total RNA isolated from various mouse tissues or cultured cells was used. Isolated RNA at first underwent deoxyribonuclease I treatment and the first strand cDNA synthesis as it was previously described (3.2.3.5.-6.). The following PCR employed Red Taq™ Genomic DNA Polymerase purchased from Sigma and specific to mPKDREJ (RT-PCR_2_f / RT-PCR_2_r; RT-PCR_beg_f / RT-PCR_beg_r) or ß-actine (RT-PCR_actin_f / RT-PCR_actin_r) primer pairs. PCR mixture contained 50 ng template cDNA, 200 µM dNTP mix, 300 nM of each primer, 2.5 µl 10× reaction buffer, $_{dd}H_2O$ to 24 µl and 1 µl (1 unit) Red Taq™ Polymerase. PCR conditions for PKDREJ were 30 cycles at 94°C for 15 sec, 59°C for 30sec and 72°C for 30sec, for β-actin – 23 cycles 94°C for 15 sec, 55°C for 30sec and 72°C for 30sec. The resulting PCR products were analysed on a 1% agarose gel and visualized by ethidium bromide staining.

3.2.3.8. Site-directed mutagenesis

All site-directed mutagenesis procedures were performed using the XL QuickChange Mutagenesis kit (Stratagene) according the protocol of the manufacturer.

3.2.3.9. Bacterial two-hybrid screening

For bacterial two-hybrid screening of mouse testis cDNA library BacterioMatch™ Two-Hybrid System XR Plasmid cDNA Library (Stratagene) was employed. Screening was performed with PKDREJ C-terminus (2050-2126 aa) as well as with PLAT domain (1090-1233 aa) subcloned into the pBT bait plasmid vector. Both two-hybrid experiments were carried out according the protocol of the manufacturer without significant modifications.

3.2.3.10. Molecular cloning strategies

The mouse PKDREJ cDNA fused through the unique EcoRI restriction site with yellow fluorescence protein (YFP) on its carboxy-terminus (further PKDREJ-YFP) was kindly provided by Dr. Zinpeng Li and used as a basis for all PKDREJ plasmid constructs. All PKDREJ cDNA constructs were confirmed by sequencing and identified mutations were successfully corrected by site-directed mutagenesis.

Generation of PKDREJ-CFP construct

In the PKDREJ-YFP construct the C-terminally fused YFP-cDNA was replaced by the cDNA of the cyan fluorescent protein (CFP) in the PKDREJ-YFP construct using the unique EcoRI restriction site on the cDNA and the AvrII restriction site on the vector.

Generation of the truncated PKDREJ mutant – PKDREJΔ(20-1023)

The N-terminally truncated version of PKDREJ, PKDREJΔ(20-1023), was constructed in two steps. First, an EcoRI restriction site was introduced directly after the signal sequence (61-66 bp) through site-directed mutagenesis. The second step included PCR-amplification of the C-terminus (3064-6381 bp) utilizing a forward primer sPJ-PCR_f containing an EcoRI restriction site and a nucleotide sequence encoding the FLAG-tag (GAC TAC AAG GAT GAC GAC GAT AAG) and the reverse primer sPJ-PCR_r containing TAA-stop-codon. The PCR product was inserted into the pcDNA3.1

vector using the pcDNA3.1/V5-His TOPO TA expression kit and subsequent subcloning of the signal sequence into the EcoRI restriction site was performed. The C-terminally fused YFP or CFP cDNAs were subcloned from corresponding PKDREJ constructs into PKDREJΔ(20-1023) using a Bpu1102I (at the position 3804) recognition site in the cDNA and an AvrII restriction site in the vector.

Generation of the wild-type PKDREJ

YFP-tag in the PKDREJ-YFP construct was substituted with TAA stop-codon from PKDREJΔ(20-1023) construct using the AvrII restriction site in the vector and subsequent partial digest at the Bpu1102I (at 3804 bp) recognition site in the cDNA.

Subcloning of PKDREJΔ(20-1023) into pOG-I vector

The cDNA of PKDREJΔ(20-1023) inserted in pcDNA 3.1 was amplified by PCR using ClaI_f forward primer containing ClaI restriction site and AatII_r reverse primer containing AatII restriction site. After separation on 0.8% agarose gel the PCR product was inserted into empty pcDNA 3.1 vector using the TOPO-TA Expression Kit (Invitrogen) and subsequent subcloning of PKDREJΔ(20-1023) cDNA into multiple cloning site of pOG-I vector through ClaI and AatII restriction sites was performed.

Subcloning of PKDREJ into pOG-I vector

Subcloning of PKDREJ into pOG-I vector was performed by two steps. In the first step ClaI restriction site was introduced into multiple cloning site of pcDNA 3.1 vector (position 911-916 bp) directly in front of PKDREJ cDNA by site-directed mutagenesis using mutagenesis primer pair ClaI_mut_f / ClaI_mut_r. After restriction with ClaI and partial digest with Bpu1102I (at 3804 bp) N-terminal part of PKDREJ was subcloned to PKDREJΔ(20-1023) construct in pOG-I vector.

Subcloning of PKDREJ into pIND/Hygro vector

To subclone PKDREJ-WT into pIND/Hygro vector the vector multiple cloning site was modified by introducing ClaI restriction site at the position 549-553 bp by site-directed mutagenesis using mutagenesis primer pair pIND-ClaI_f / pIND-ClaI_r. Afterwards the PKDREJ cDNA was subcloned into pIND/Hygro from pOG-I vector using ClaI and NotI restriction sites.

Generation of PKDREJ GST-fusions

All GST-fusion constructs were created in pGEX-4T-1N vector using EcoRI and XhoI restriction sites. Three parts of PKDREJ – N-terminal (253-495 bp), Loop (4890-5200 bp) and C-terminal parts (6148-6381 bp) – were amplified by touch-down PCR using primer pairs GST-N-term_f / GST-N-term_r, GST-Loop_f / GST-Loop_r, GST-C-term_f / GST-C-term_r respectively. All forward primers contained EcoRI recognition site and all reverse primers included XhoI restriction site. After separation on 1% agarose gel the PCR products were cut out of the gel, DNAs were purified with QIAEX® II Gel Extraction Kit, solved in $_{dd}H_2O$, digested with EcoRI and XhoI for 1 hour at 37°C and separately subcloned into pGEX-4T-1N vector.

3.2.4. Biochemical methods

3.2.4.1. Membrane protein preparation

Cells growing in a culture flask or dish were washed twice with ice-cold PBS and scraped or resuspended in lysis buffer. After 20 min incubation on ice cells were homogenized by forcing the cell suspension six to ten times through a 0.5 mm × 25 mm needle attached to a disposable syringe. The lysate was then centrifuged at 1500 g for 10 min at 4°C to pellet debris and organelles. The supernatant was carefully collected and centrifuged at 100000 g for 1 hour at 4°C. The membrane pellet was solved in the lysis or other appropriate buffer for further experiments.

Lysis buffer

Tris/HCl (pH 7.5)	25 mM
EDTA	1 mM
1 tablet “Complete Mini” protease inhibitor cocktail to 7 ml of volume	

Solubilization buffer

Tris-base (pH 9.5)	20 mM
Urea	7 M
Thiourea	2 M
Chaps	4 % (w/v)
Triton X-100	1 % (v/v)

DTT	1 % (w/v)

1 tablet “Complete Mini” protease inhibitor cocktail to 7 ml of volume

3.2.4.2. Expression of GST-fusion proteins in *E.coli*

For the expression of GST-fusion proteins protease deficient BL21 *E.coli* strain was used. Competent BL21 cells were transformed with a few µg of pGEX-4T-1N vector containing GST-fusion cDNA. Next day at least 83 ml of overnight bacterial culture were mixed 1:3 with complete LB medium and grown additional hour at 37°C prior to induction with 0.2 mM IPTG. After 3 hour of induction suspension was centrifuged at 5000 rpm for 10 min, the pellet was resuspenden in 25 ml of lysis buffer, sonicated 2 time for 30 sec at full power and subsequently centrifuged once again at 5000 rpm for 5 min. Clear supernatant was collected in a separate tube and incubated for 30 min on a rocker with 150 µl of GSH beads preliminary equilibrated in lysis buffer. Then the beads were washed 3 times in lysis buffer but with 0.5 % Triton X-100 and without DTT and used for further analysis by SDS-PAGE.

Lysis buffer

Tris-base (pH 8.0)	20 mM
NaCl	100 mM
EDTA	1 mM
Triton X-100	1 % (v/v)
DTT	10 mM

3.2.5. Immunological methods

Amount of antibodies used in different experiments are indicated in Table 3.2.

Table 3.2. Concentrations of antibodies used in present study

Name of antibodies	**Concentration for**		
	IC/IH*	**WB***	**IEM***
Anti-PKDREJ, N-terminus, Ab36	3 µg/ml	4 µg/ml	6 µg/ml
Anti-PKDREJ, Loop, Ab47	4 µg/ml	5 µg/ml	—
Anti-PKDREJ, C-terminus, Ab46	3 µg/ml	4 µg/ml	—
Alexa Fluor® 488, anti-rabbit IgG	1 µg/ml	—	—

Alexa Fluor® 546, anti-rabbit IgG	1 μg/ml	—	—
Monoclonal Anti-Tubulin, acetylated	1:4000	—	—
Anti-mouse IgG, FITC conjugate	1:400	—	—
Polyclonal Anti-Green Fluorescent Protein	—	1:1000	—
Anti-rabbit IgG, horseradish peroxidase conjugate	—	1:5000	—
EM anti-rabbit IgG, 10 nm gold conjugate	—	—	1:100
Anti-GST, horseradish peroxidase conjugate	—	1:5000	—

* IC/IH – immunocytochemistry/immunohystochemistry; WB – Western-blot; IEM – immunoelectron microscopy

3.2.5.1. Generation of anti-PKDREJ antibodies

Mouse PKDREJ amino acid sequence was analyzed with the "DNA Star" software and three different peptides were chosen for rabbit immunization (Table 3.3.). The main criteria for epitopes design were: 1) high antigenic index, 2) high hydrophilicity, 3) high charge and surface probability and 4) low probability of any second polypeptide structure. Chosen peptides were analysed for probable homology to any other proteins and no significant matches were found. After synthesis and before immunization peptides were covalently coupled to the keyhole limpet hemocyanin. Finally, affinity purified polyclonal rabbit antibodies against the PKDREJ protein were produced by Eurogentec (Belgium).

Table 3.3. PKDREJ epitopes designed for immunization

1. N-terminus, 110-126 aa, (Ab36) – NRKDQNAPLILSRDEEA
   Predicted localization – extracellular
   No significant identity to any other mammalian PKDREJ

2. Extracellular loop, 1712-1727 aa, (Ab47) – SVWSKAGKQSTDKASH
   Predicted localization – extracellular
   No significant identity to any other mammalian PKDREJ

3. C-terminus, 2100-2115 aa, (Ab46) – QPEKNTRRFLGLKARN
   Predicted localization – intracellular
   Identity to bovine PKDREJ () – 81% (13/16), positives – 93% (15/16)
   Identity to human PKDREJ (NP_006062.1) – 75% (12/16), positives – 87% (14/16)

mPKDREJ	QPEKNTRRFLGLKARN
bPKDREJ	QPEKN+RR+LGLK RN
hPKDREJ	QPEKN+ R+LGLK RN

3.2.5.2. Immunocytochemistry of mouse sperm

Freshly isolated caudal epididymal mouse sperm were spotted onto glass slides and air dried. Then the cells were fixed in 4% (w/v) formaldehyde solution for 10 min or for some experiments in ice-cold acetone for 20 min. If antibody against intracellular epitope (C-terminal) were used cells were additionally permeabilized with 0.1% Triton X-100 in PBS for 10 min. After 2 hours of blocking with 10% (v/v) goat serum in PBS-T, the slides were incubated at 4°C overnight with primary antibody diluted in blocking solution. In some cases primary antibody were preincubated for several hours at room temperature with 2 µM competing peptide to assess specific binding. Next day the samples were rinsed in PBS-T (3 × 5 min) and incubated with 1 µg/ml Alexa Fluor 488 goat anti-rabbit IgG and 5 µg/ml propidium iodide diluted in blocking solution for 1 hour at room temperature. After three additional washes in PBS-T, slides were mounted in DacoCytomation fluorescent mounting medium (DAKO) and examined with the inverted Zeiss LSM 510 META laser scanning confocal microscope using the Plan-Apochromat 63×/1.4 oil objective. Excitation wavelengths 488/545 of argon/neon lasers and emission filters 500-530 and >560 nm were used for detection of Alexa Fluor 488 conjugates and propidium iodide, respectively.

3.2.5.3. Immunocytochemistry of adherent cells

For immunocytochemical experiments HEK293, COS7, GC-1, GC-2 and primary aortic smooth muscles cells were grown on glass coverslips. Prior to fixation culture medium was aspirated and cells were washed twice with PBS. Afterwards cells were fixed in 4% (w/v) formaldehyde solution for 10 min, rinsed twice with PBS and permeabilized with 0.1% Triton X-100 in PBS for 10 min if necessary. Further steps starting from blocking were performed as previously described (3.2.5.2.).

3.2.5.4. Immunohystochemistry

Freshly isolated mouse tissues were embedded in Tissue-Tek® and snap-frozen at -40°C. Frozen tissues were sectioned in a cryostat (thickness 5 µm), fixed in acetone at

4°C for 20 min and preceded with blocking and antibody incubations as it described above (3.2.5.2.).

3.2.5.5. Immunoelectron microscopy

Freshly isolated mouse spermatozoa were fixed for 10 min in immunofixation solution (1.25 % paraformaldehyde, 0.5 % glutaraldehyde, 0.025 % picric acid in 0.05 M cacodylate buffer), washed thoroughly with PBS and subsequently gently shaked for 2 hours at room temperature in blocking solution containing 10 % (v/v) goat serum in PBS. Thereafter, cells were incubated overnight at 4°C with the primary anti-PKDREJ antibody (Ab 36, 6 µg/ml) diluted in blocking solution. After three washes with PBS, a 1:100 dilution of a goat 10 nm gold-conjugated goat anti-rabbit IgG was applied for 2 hours at room temperature. After removing the secondary antibody by three washes with PBS, cells were refixed for 24 hours at 4°C with Ito-fixation solution (Forssmann et al., 1977), washed with 0.1 M sodium cacodylate solution (pH 7.3) and subsequently stained for 1 hour at room temperature with a solution containing 1 % osmium tetroxide and 1.5 % potassium ferrocyanide. After three additional washing steps with the sodium cacodylate buffer, the sperm pellet was dehydrated with ascending ethanol solutions (50, 70, 90, 96, and 100 %; 5 min each). Subsequently, the pellet was soaked with propylene oxide and propylene oxide/Epon C (1:1) for 24 hours, and then polymerized at 60°C overnight. Ultrathin sections (50 nm) were cut with a diamond knife on an Reichert ultramicrotome and were stained with 4% uranyl acetate (aqueous solution), followed by alkaline lead citrate according to Reynolds (Reynolds, 1963). Sperm ultrastructure was examined by transmission electron microscopy using Zeiss-EM 10C 902 electron microscope at 60 kV.

Immunofixation solution (pH 7.2)

Sodium cacodylat	50 mM
Paraformaldehyde	1.25 % (v/v)
Glutaraldehyde	0.5 % (v/v)
Picric acid	0.025 % (v/v)

3.2.5.6. Western immunoblotting

After voltage-clamp measurements, 10 oocytes for each injected cRNA construct as well as non-injected oocytes were placed in 300 µl ice-cold lysis buffer for 10 min and then homogenized by pipeting through a 200 µl tip. To pellet the cell debris, lysates were centrifuged at 13000 × g at 4°C for 20 min. Subsequently, supernatants were carefully transferred to a separate tube. 40 µl of each oocytes lysate were mixed with 10 µl of 5 × SDS sample buffer and 1 µl of β-mercaptoethanol and thereafter incubated at room temperature for 15 min. The same procedure was used for lysates of HEK293 cells growing in 35-mm dishes. To separate the protein samples, SDS polyacrylamide gel electrophoresis (6 % [v/v]) was performed using the Laemmli buffer system (Laemmli, 1970). After separation, proteins were transferred overnight to PVDF membrane in a wet-electrophoresis chamber at 20 V. Next day the transfer was controlled by staining the membrane with Ponceau-S and afterwards unspecific binding sites were blocked by incubating membranes with 5 % non-fat dry milk in PBS-T for 2 hours at room temperature. Subsequently, anti-PKDREJ antibody used at a concentration of 4 µg/ml as well as anti-green fluorescent protein antibody diluted 1:1000 were applied at 4°C overnight. Thereafter, membranes were washed three times for 5 min with PBS-T and incubated with the secondary goat anti-rabbit IgG/horseradish peroxidase conjugate at room temperature for 1 hour. Subsequently, membranes were rinsed again with PBS-T (3 × 5 min), and the signal was detected using ECL reagent (Amersham Bioscience).

Lysis buffer

NaCl	150 mM
Tris-base (pH 7.5)	20 mM
Triton X-100	1 %

1 tablet “Complete Mini” protease inhibitor cocktail to 7 ml of volume

3.2.6. Reproducibility of results

All experiments were performed independently at least three times and the representative one is shown.

4. RESULTS

4.1. PKDREJ Expression in Mouse Testis in Spermatogenic Cells

The first objective of the present study was to evaluate the tissue distribution of PKDREJ. Therefore, multiple mouse tissue northern blot analysis was performed with a labelled PKDREJ cDNA probe. The probe hybridized predominantly to a transcript of 8 kb derived from mouse testis but a weak signal was also observed in lung. No significant signal was detectable in other tissues (Fig. 4.1.).

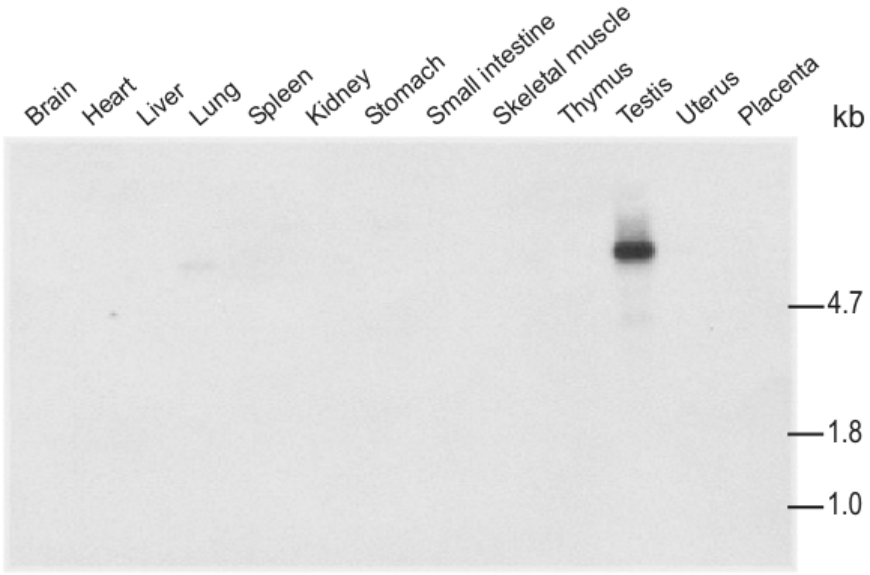

Figure 4.1. PKDREJ expression in mouse testis demonstrated by Northern blot analysis
Northern blot of mouse adult tissue total RNA was hybridized with murine PKDREJ cDNA probe. A transcript of about 8 kb is detectable in mouse testis and lung.

The expression of PKDREJ mRNA in testis was confirmed by RT-PCR. Since PKDREJ gene contains only one exon there was no possibility to design a PCR primer pair allowing discrimination between amplification of cDNA and genomic DNA, which minor contaminants are often present in RNA samples. Therefore, total RNA was subjected to deoxyribonuclease I treatment prior to reverse transcriptase reaction to remove genomic DNA. As an additional negative control RNA sample after DNAse treatment but without first cDNA strand was used for PCR reaction. Under these conditions, we could detect PKDREJ mRNA expression in testis but we were unable to amplify PKDREJ cDNA from total RNA isolated from two immortalized mouse germ

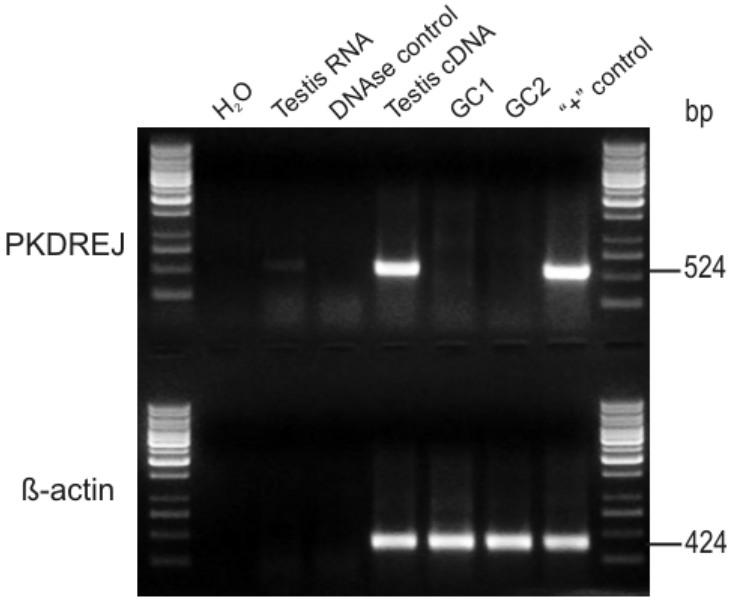

Figure 4.2. PKDREJ expression in mouse testis confirmed by RT-PCR

Diagnostic RT-PCR for PKDREJ mRNA expression in mouse testis and germ cell lines GC-1 and GC-2. Total RNA was isolated from mouse testis and germ cell lines GC-1 and GC-2, and exposed to DNAse treatment prior cDNA synthesis. Equal amounts of testis RNA before and directly after DNAse treatment (DNAse control) were used as negative controls for PCR. cDNA prepared from PKDREJ inducible cell line served as positive control ("+" control).

cell lines, GC-1 and GC-2, which are believed to represent spermatogonia Type B (Hofmann et al., 1992) and early spermatids (Hofmann et al., 1994), respectively (Fig. 4.2.).

Since testis as a tissue is composed of various cell types we addressed the question which population of testicular cells contains PKDREJ transcript. In cooperation with Klaus Steger (Department of Urology and Pediatric Urology, Justus Liebig University, Giessen) *in situ* hybridization on sections of adult mouse testis with PKDREJ-specific probe was performed. Figure 4.3. illustrates strong labelling of seminiferous tubules reflecting staining of spermatogonia distributed along the outer edge of seminiferous tubules and pachytene spermatocytes and round spermatids towards the tubule lumen. Other cell types including peritubular cells, Sertoli cells and interstitial Leydig cells did not show any specific hybridization signal, and the sense probe failed to label any testicular cells (Fig. 4.3.). This finding prompted us to conclude that PKDREJ expression in testis is germ cell-specific.

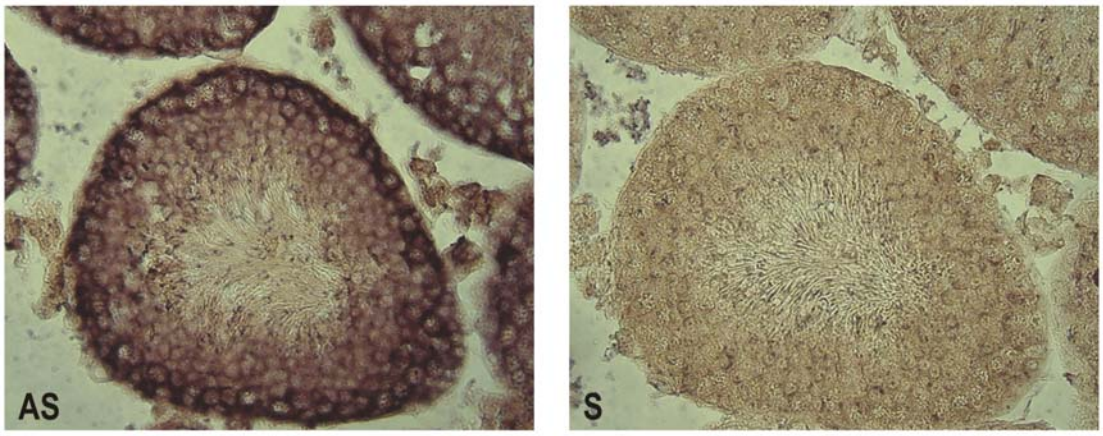

Figure 4.3. PKDREJ expression in spermatogenic cells demonstrated by *in situ* hybridization of mouse testicular tissue

In situ hybridization on two consecutive paraffin sections showing a murine seminiferous tubule. While the sense probe **(S)** is negative for Pkdrej mRNA, the antisense probe **(AS)** exhibits a strong signal in spermatogonia and spermatocytes and a weak signal in round spermatids (original magnification × 63).

4.2. Heterologous Expression of PKDREJ

Considering that PKDREJ is a membrane protein possibly functioning as an ion channel or receptor we overexpressed it in various heterologous expression systems to investigate its subcellular localization and come close to its function.

First, we transiently expressed the PKDREJ C-terminally fused to YFP and introduced into pcDNA3.1 expression vector in HEK293 cells because they are easy to maintain and to transfect and many signal transduction proteins were successfully overexpressed there. Confocal laser scanning microscopy of living cells revealed PKDREJ-YFP to be mainly localized within intracellular membrane compartments (Fig. 4.4. A). In addition we noted that the recombinant full-length protein could only be expressed at very low level and many positive cells appeared atypical morphology like undergoing apoptosis.

Recently it was reported that proteolytic cleavage of latrophilin within its N-terminal GPS domain required for delivery of the receptor to the cell membrane and the two fragments behave as independent proteins which associate upon ligand binding (Volynski et al., 2004). To examine the impact of N-terminal cleavage and truncation on cellular protein targeting, we generated two PKDREJ variants: a GPS-domain mutant

PKDREJ(H1037R) and an N-terminally truncated PKDREJΔ(20-1023) variant, both C-terminally fused to YFP. In transiently transfected HEK293 cells, the subcellular localization of both PKDREJ mutants was intracellular and similar to that observed with the wild-type protein (Fig. 4.4. B and C).

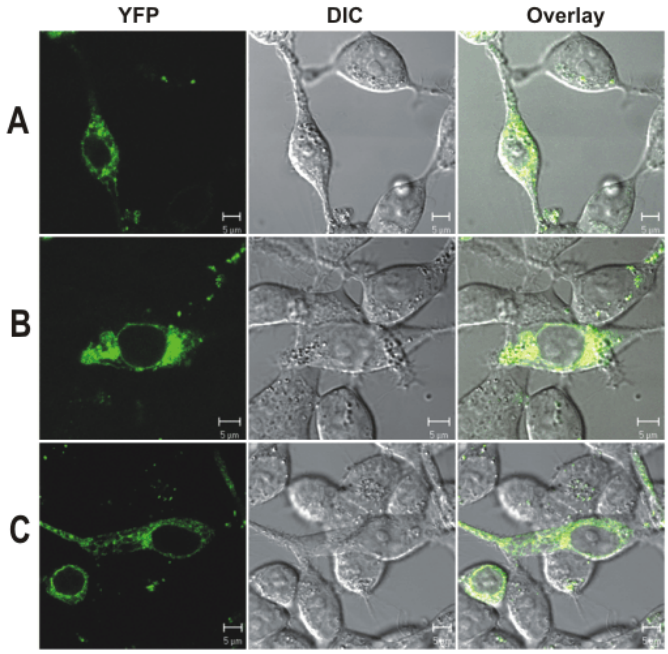

Figure. 4.4. Subcellular localization of PKDREJ in transiently transfected HEK293 cells
Wild type PKDREJ **(A)**, GPS-site mutated PKDREJ(H1037R) **(B)** and N-terminally truncated PKDREJΔ(20-1023) **(C)** were C-terminally fused to YFP and transiently expressed in HEK293 cells. Confocal images of YFP fluorescence (YFP), the corresponding differential interference contrast (DIC) images of live cells, and overlays of both are depicted (scale bars 5µm).

To exclude that intracellular retention of recombinant PKDREJ is a unique property of HEK293 cells we changed the heterologous expression system to COS7 cells. The subcellular distribution of PKDREJ C-terminally fused to YFP transiently expressed in COS7 cells was not on the plasma membrane rather in intracellular membrane compartments like observed in HEK293 cells (Fig. 4.5. A).

It is known that some membrane proteins require tissue-specific adaptors or partners for their proper subcellular trafficking. Since PKDREJ is expressed in spermatogenic cells immortalized germ cell lines GC-1 and GC-2 could be the heterologous system of choice. By nuclear electroporation we transfected both spermatogenic cell lines with PKDREJ-YFP cDNA. The subcellular localization of PKDREJ in GC-1 and GC-2 bore a resemblance with that observed in HEK293 and COS7 cells (Fig. 4.5. B and C). We also noticed a very low level of transfection

efficacy and high cell mortality after transfection with PKDREJ-YFP construct while with YFP alone the efficiency was 75-80% and almost no mortality. This phenomenon can be a result of the PKDREJ toxicity manifesting in overexpression system.

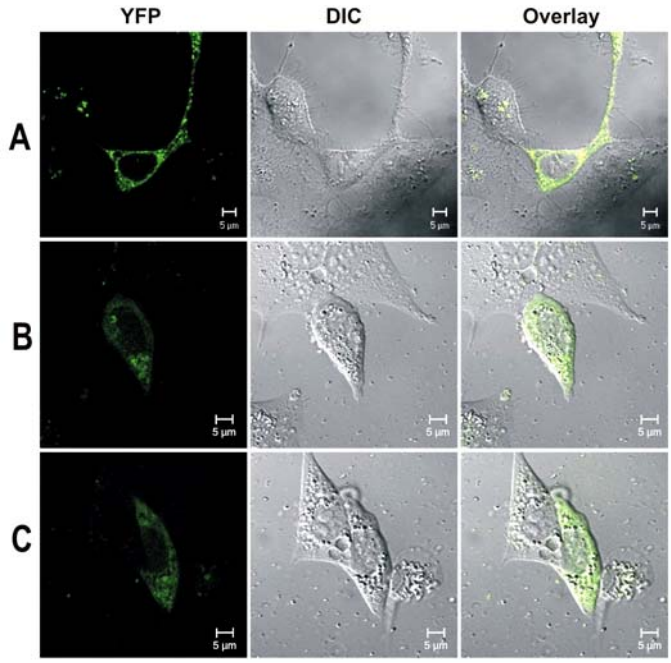

Figure. 4.5. Subcellular localization of PKDREJ in transiently transfected COS7, GC-1 and GC-2 cells

Wild type PKDREJ was C-terminally fused to YFP and transiently expressed in COS7 **(A)**, GC-1 **(B)** and GC-2 **(C)** cells. Confocal images of YFP fluorescence (YFP), the corresponding differential interference contrast (DIC) images of alive cells, and overlays of both are shown (scale bars 5µm).

It has been reported that the co-assembly of PKD1 and PKD2 is required for the formation of a functional cation channel at the cell membrane (Hanaoka et al., 2000). Furthermore, suPC2, a PKD2 homolog, associates with suREJ1, a PKD1 homolog (Neill et al., 2004), and both proteins co-localize in the plasma membrane over the acrosome of sea urchin sperm. Therefore, we co-expressed PKDREJ with human PKD1 or PKD2 proteins, which cDNAs were kindly provided by Gregory Germino and Terry Watnick (Division of Nephrology, Department of Medicine, Johns Hopkins University School of Medicine, Baltimore, USA). In these experiments despite the extremely low signal intensity we did not observed any changes in PKDREJ subcellular distribution comparing with when it is expressed alone (Fig. 4.6. A and B). As PKD2L2 (TRPP5) is the only TRPP family member whose expression is restricted to kidney, heart and testis, we also co-expressed PKDREJ constructs and mouse PKD2L2 in HEK293 cells. However, the intracellular localization of PKDREJ remained unchanged (Fig. 4.6. C).

Along these lines, co-expression of HSP70, a male germ cell-specific heat shock protein serving as a cellular chaperone, was without effect on the cellular distribution of recombinant PKDREJ (Fig. 4.6. D).

Finally, we also tested whether *Xenopus laevis* oocytes would be an adequate heterologous expression system. Subsequent to injections of oocytes with cRNAs coding for PKDREJ and its mutants we did not obtain evidence arguing for plasma membrane insertion by two-electrode voltage-clamp measurements.

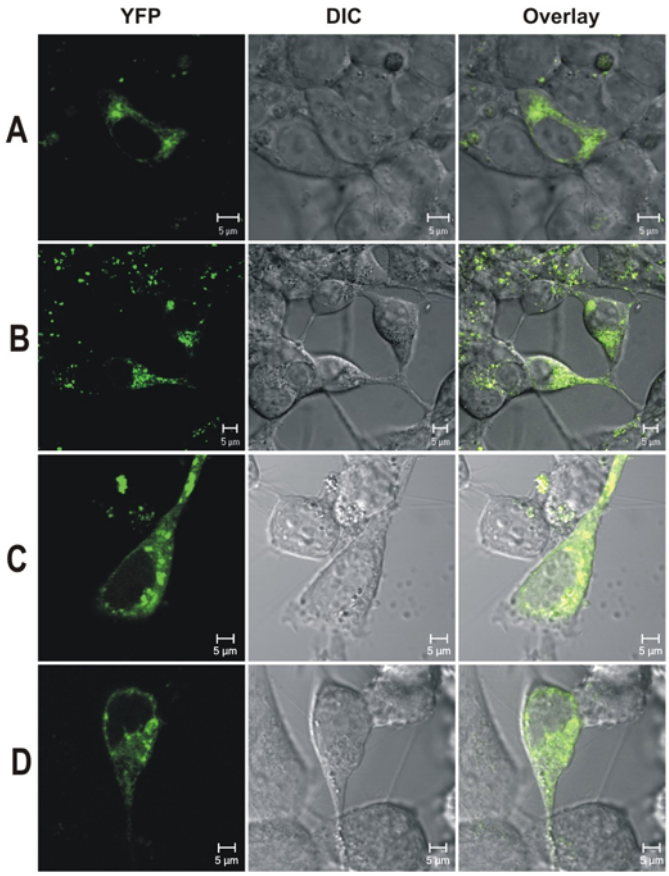

Figure. 4.6. Subcellular localization of PKDREJ co-expressed with hPKD1, hPKD2, mPKD2L2 or mHSP70 in transiently transfected HEK293 cells

PKDREJ C-terminally fused to YFP was co-expressed with wild type human PKD1 **(A)**, human PKD2 **(B)**, murine PKD2L2 **(C)** or HSP70 **(D)** in HEK293 cells. Confocal images of YFP fluorescence (YFP), the corresponding differential interference contrast (DIC) images of alive cells, and overlays of both are shown (scale bars 5µm).

4.3. Generation and Characterisation of PKDREJ-specific Antibodies

To see whether fusion with YFP would influence the cellular localization of recombinant PKDREJ and to directly visualize PKDREJ at the protein level, we generated polyclonal rabbit antibodies against a 17-amino acids synthetic peptide derived from the N-terminus of the protein. The final antiserum was affinity-purified with the peptide used for immunisation, and the specificity of antibodies was subsequently determined by ELISA (Eurogentec).

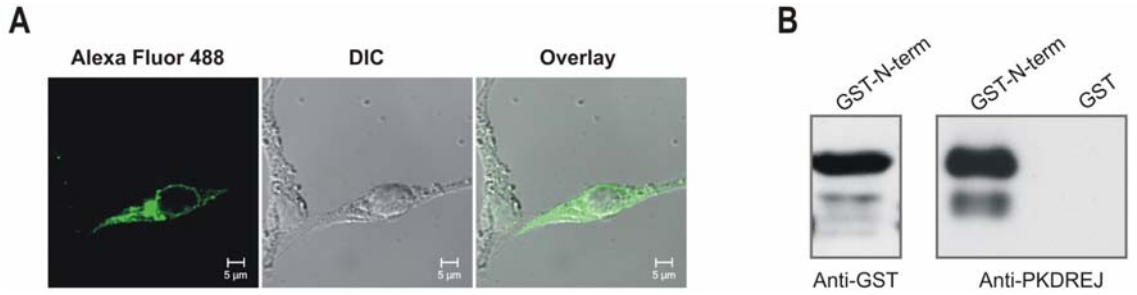

Figure. 4.7. Characterisation of anti-PKDREJ antibodies

(A) Immunostaining of fixed HEK293 cells transiently transfected with wild type PKDREJ cDNA using PKDREJ-specific antibodies. Whereas untransfected cells remain unstained, bright signal in positive cells is observed. Confocal image of Alexa Fluor 488 fluorescence, the corresponding differential interference contrast (DIC) image of fixed cells, and overlay are shown (scale bars 5µm). **(B)** Immunoblots with PKDREJ N-terminus fused to GST stained with anti-GST or anti-PKDREJ antibodies.

In fixed HEK293 cells transiently transfected with wild-type PKDREJ in pcDNA3.1 vector, the antibodies labelled positive cells without producing significant background (Fig. 4.7. A). In line with the results obtained in living cells, PKDREJ immunoreactivity was not detectable at the plasma membrane, but was localized intracellularly displaying a fine reticular cytoplasmic pattern reminiscent of the endoplasmatic reticulum.

Next, we generated a GST-fusion where N-terminal part of PKDREJ containing the epitope used for antibodies production was subcloned to the C-terminus of GST in pGEX vector. After expression the construct in BL21 *E.coli* and purification of the GST-fusion it was subjected to SDS-PAGE and immunoblot with both anti-GST and anti-PKDREJ antibodies. The anti-PKDREJ antibodies detected specifically the fusion protein but did not show any immunoreactivity to GST alone (Fig. 4.7. B).

There are observations that some genes can be expressed in heterologous systems more efficiently when introduced in pIRES vectors. We subcloned wild-type PKDREJ and its N-terminally truncated variant PKDREJΔ(20-1023) into pIRES-EGFP expression vector containing the internal ribosome entry site between the multiple cloning site and enhanced green fluorescent protein (EGFP) coding region. To determine subcellular localization of PKDREJ proteins expressed in pIRES vector we performed immunocytochemistry with transiently transfected HEK293 cells. As it was

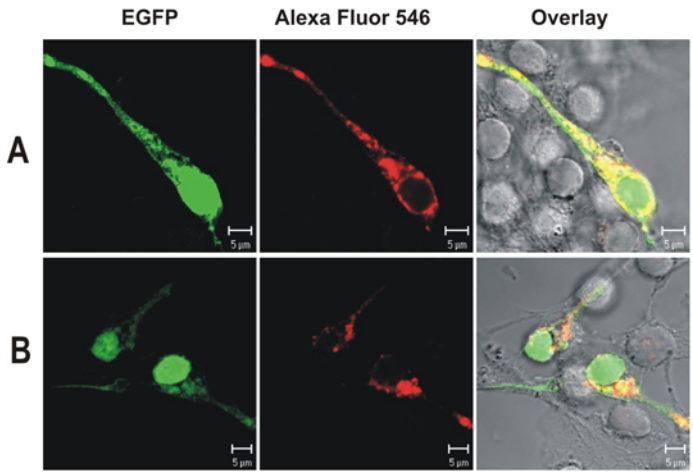

Figure. 4.8. Subcellular localization of PKDREJ expressed in pIRES-EGFP vector in transiently transfected HEK293 cells

Wild type PKDREJ **(A)** and N-terminally truncated PKDREJΔ(20-1023) **(B)** were subcloned into pIRES-EGFP vector, transiently expressed in HEK293 cells and immunostained with anti-PKDREJ antibodies (red signal). Confocal images of EGFP fluorescence, Alexa Fluor 546 fluorescence and overlays of both with the corresponding differential interference contrast images of fixed cells are depicted (scale bars 5µm).

reported previously the anti-PKDREJ antibodies recognized specifically positive cells but no changes were observed in the distribution of PKDREJ and its mutant comparing with expression in pcDNA3.1 vector (Fig. 4.8.). In all cases PKDREJ was predominantly localized within intracellular endoplasmatic compartments whereas clear plasma membrane localization was never observed.

4.4. Generation of PKDREJ-inducible cell line

While overexpressing PKDREJ in heterologous systems we faced several restrictions limiting functional studies of PKDREJ in a cellular model. These included:

i) poor transfection efficiency; ii) low level of the protein expression; iii) probable cytotoxicity. To overcome these difficulties we generated PKDREJ inducible cell line taking the advantage of ecdysone-inducible mammalian expression system. EcR293 cells were transfected with wild-type PKDREJ in pIND/Hygro expression vector, 26 individual stable clones were selected, propagated and checked by RT-PCR for ability to express PKDREJ in response to Ponasterone A. To be sure that the full-length PKDREJ cDNA is integrated into a cell genome we performed RT-PCR with primer pairs to both 5´- and 3´-ends. After this screening step only 4 clones were concluded to be PKDREJ positive. These were additionally tested for their ability to be induced with different concentrations of Ponasterone A by performing RT-PCR with low number of cycles. Although the basal level of PKDREJ expression was always observed in all 4 clones we detected increase of PKDREJ expression in response to Ponasterone A. The information concerning PKDREJ-inducible clones is summarized in Table 4.1.

Table 4.1. Characterisation of PKDREJ-inducible clones

	1.1	5.1	6.4	7.2
PCR 3´Primers	+	+	+	+
PCR 5´Primers	+	+	+	+
Induction (RT-PCR)	+	++	++	+
Induction (Western)	not performed	+	+	not performed

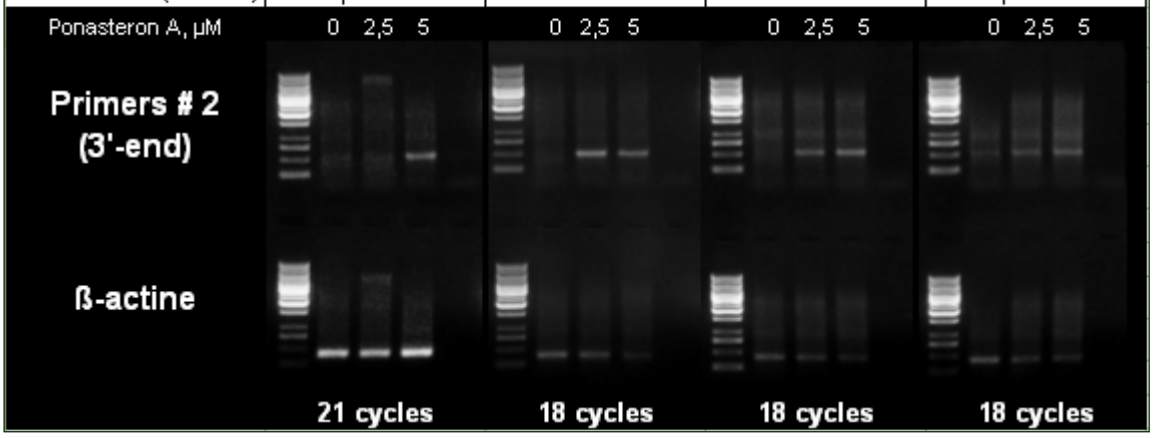

As a rule the level of protein expression in inducible cell line is much lower than while transient expression. Therefore, we addressed the issue whether the expression of PKDREJ in our inducible cell lines can be detected on the protein level. In the Western-blots with total cell lysates prepared in 24 hour after Ponasterone A induction we could disclose a weak specific band of about 240 kDa corresponding the full-length PKDREJ protein despite a band of unknown nature of about 130 kDa as well as several unspecific

bands were also observed (Fig. 4.9.). The unknown band seems to be a product of unspecific proteolysis but not GPS cleavage since the calculated molecular mass of the clef PKDREJ N-terminus would be 115 kDa.

To detected PKDREJ expression in inducible cells on the protein level we also performed immunocytochemistry with induced and non-induced cells but no significant difference in staining pattern was detected. Similar to transient expression we did not observe typical plasma membrane PKDREJ staining in inducible cells.

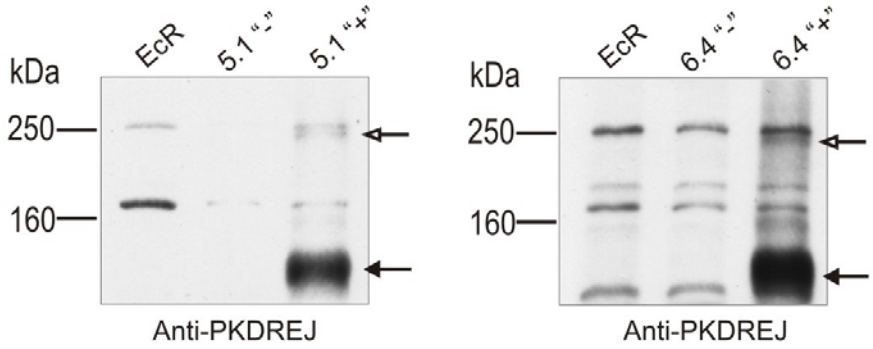

Figure. 4.9. Expression of PKDREJ in inducible clones 5.1 and 6.4 demonstrated by Western-blot
Cells (5.1 "+"; 6.4 "+") were induced for 24 hours with 5 µM Ponasteron A and whole cell lysates were subjected to Western-blot analysis with PKDREJ-specific antibodies. Basic EcR cells and non-induced cells (5.1 "-"; 6.4 "-") served as negative controls. White arrows indicate full-length PKDREJ of about 240 kDa. Black arrows point a band of unknown nature.

4.5. Lack of the PKDREJ Cleavage at the GPS Domain in Heterologous Expression Systems

Two plasma membrane proteins, suREJ3 and PKD1, which are homologs of PKDREJ, have recently been shown to be proteolytically processed at the GPS domain (Mengerink et al., 2002; Qian et al., 2002). In order to test whether PKDREJ is cleft as well in the extracellular domain, we examined wild-type PKDREJ and an engineered variant harbouring a mutation in the GPS domain. Primary sequence alignment of several proteins containing GPS domains revealed a highly conserved cleavage motif that is modified by the insertion of an additional H residue (H1039) in the case of PKDREJ (s. Fig. 1.3. C). We introduced a missense mutation to generate PKDREJ(H1037R). The latter H residue is localized two positions upstream of the predicted cleavage site and has been identified as a critical residue for the proteolytic processing of PKD1 (Qian et al., 2002).

In immunoblots of lysates from *Xenopus laevis* oocytes injected with both cRNAs, anti-PKDREJ antibodies detected one prominent specific band of about 240 kDa corresponding to full-length PKDREJ (Fig. 4.10. A). Shedding of an N-terminal portion of PKDREJ with a predicted molecular mass about 115 kDa was never observed even after prolonged film exposure. To exclude that the lack of proteolytic cleavage reflects a unique property of *Xenopus laevis* oocytes, we overexpressed C-terminally YFP-tagged wild-type PKDREJ and the corresponding H1037R mutant also in HEK293 cells and subjected total cell lysates to Western blot analysis with anti-GFP antibodies. In these experiments a distinct specific band representing wild-type PKDREJ fused to YFP migrated with an expected molecular mass of 270 kDa, whereas a cleft C-terminal portion of PKDREJ-YFP anticipated to migrate at about 150 kDa could never be detected (Fig. 4.10. B). Thus, so far we could not obtain any experimental evidence to support the notion that PKDREJ is proteolytically processed within the extracellular domain.

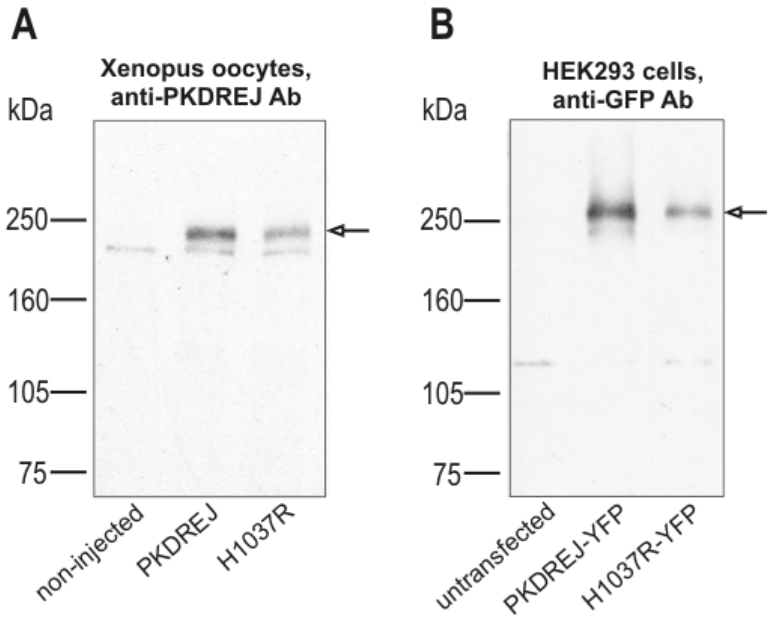

Figure. 4.10. Lack of the PKDREJ cleavage at the GPS domain in heterologous expression systems

(A) Western-blot of total lysate from *Xenopus laevis* oocytes injected with cRNAs of wild type PKDREJ or GPS-domain mutated PKDREJ construct (PKDREJ(H1037R)). PKDREJ was visualized using a PKDREJ-specific antibodies generated against an N-terminal peptide. The position of the PKDREJ-specific band of about 240 kDa is indicated by an arrow. **(B)** Western-blot of total lysate from HEK293 cells transiently expressing C-terminally fused to YFP either PKDREJ or its GPS-domain mutant in which histidine 1037 was changed to arginine (H1037R). Immunoreactivity was detected applying an anti-GFP antibodies. The position of the specific band about 270 kDa is indicated by an arrow.

4.6. Localization of PKDREJ on the Plasma Membrane of Mouse Sperm Head

Considering that PKDREJ mRNA is expressed in mouse spermatogenic cells, we addressed the question whether the protein is also present. To this end, indirect immunofluorescence experiments with cryosections of mouse testis and epididymis were performed. Slides were incubated with the primary anti-PKDREJ antibodies and counterstained with propidium iodide to visualize cell nuclei. Surprisingly, we could not

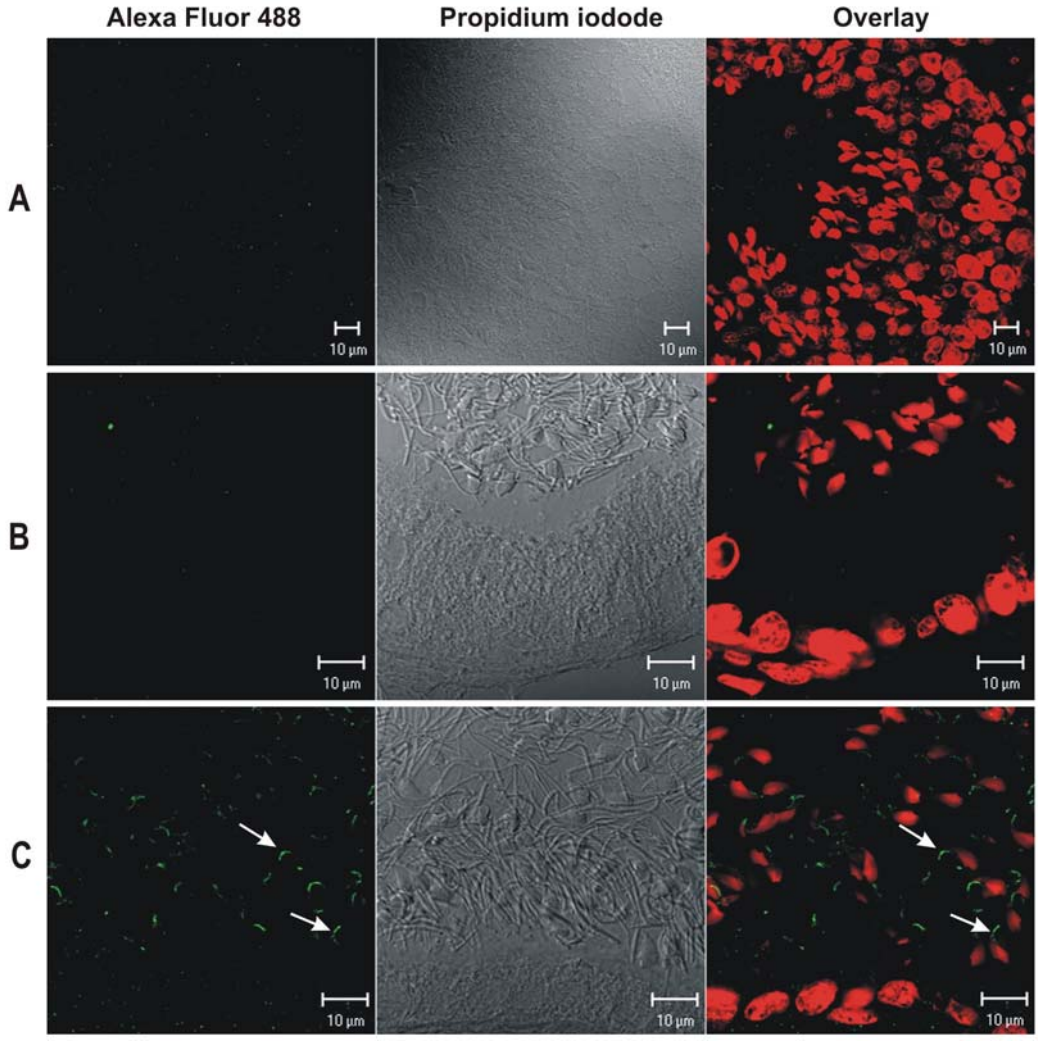

Figure. 4.11. Immunohistochemical examination of PKDREJ in mouse testis and epididymis Cryosections of mouse testis **(A)**, initial segment **(B)** and cauda **(C)** epididymis were stained with PKDREJ-specific antibodies (green signal). Cells nuclei were additionally stained with propidium iodide (red signal). Differential interference contrast (DIC) images and overlays of Alexa Fluor 488 and propidium iodide (PI) fluorescence are depicted. White arrows indicate the localization of the PKDREJ signal (scale bars 10µm).

detect any specific signal corresponding to the PKDREJ protein either in testicular germ cells (Fig. 4.11. A) or in spermatozoa within the initial segment of epididymis (Fig. 4.11. B). However, spermatozoa inside the lumen of caput, corpus and cauda epididymis were stained and signal intensity increased with sperm maturation (Fig. 4.11. C). Since spermatozoa are unable to synthesize proteins de novo, and our antibodies specifically detect recombinant PKDREJ protein (see Fig. 4.7. and 4.10.), this phenomenon more likely reflects PKDREJ processing taking place in the initial segment of the epididymis resulting in unmasking of the epitope recognized by anti-PKDREJ antibodies.

To determine the precise localization of PKDREJ in spermatozoa we performed immunocytochemistry with sperm isolated from the cauda epididymis and the vas deferens. Representative confocal images demonstrated in figure 6 show that immunofluorescence is only detectable on the sperm head in the acrosomal region and on the inner aspect of the falciform-shaped head (Fig. 4.12. A). Interestingly, the

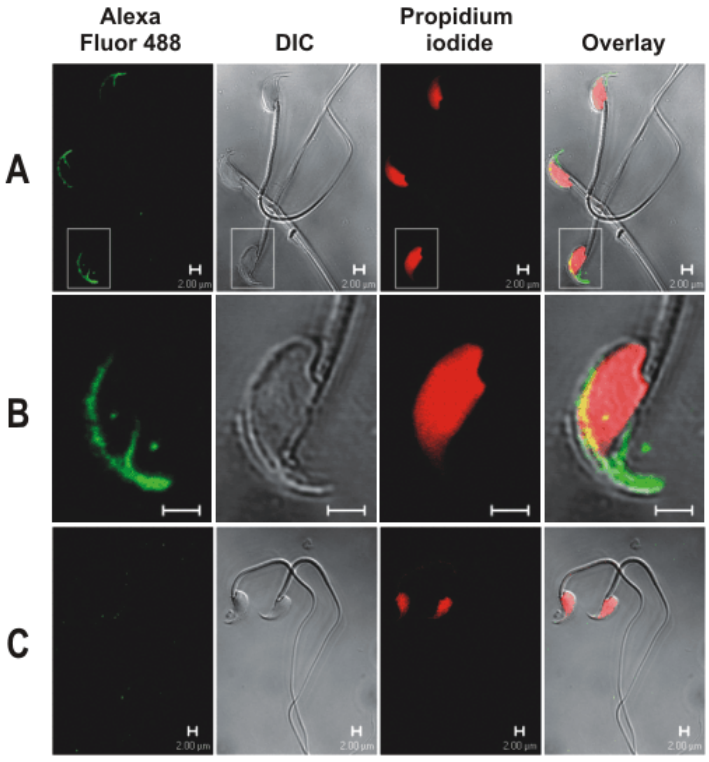

Figure. 4.12. Immunolocalization of PKDREJ in the acrosomal region and on the inner aspect of the falciform-shaped mouse sperm head

Cauda epididymal mouse spermatozoa were stained with PKDREJ-specific antibodies preincubated without **(A, B)** or with **(C)** competing peptide. Cells nuclei were additionally stained with propidium iodide. Images of Alexa Fluor 488 fluorescence, the corresponding differential interference contrast (DIC) images, propidium iodide fluorescence, and overlays are depicted (scale bars 2µm).

fluorescence signal does not completely cover the acrosomal cap but is rather located on the border between the cap and the equatorial segment as illustrated by confocal imaging at a higher magnification (Fig. 4.12. B). Preincubation of the antibodies with the competing peptide entailed the complete loss of labeling (Fig. 4.12. C).

To prove plasma membrane localization of PKDREJ in spermatozoa, we performed immunoelectron microscopy. Prior to embedding, freshly isolated mouse spermatozoa were stained with the primary anti-PKDREJ antibodies followed by incubation with the gold-labeled secondary antibodies. By analyzing ultrathin sections, we observed that the majority of gold particles are bound to the outer aspect of the plasma membrane of sperm heads (Fig. 4.13.). These results are in accordance with the predicted protein topology (s. Fig. 1.3. A), assuming that in analogy to the situation with PKD1 and suREJ3 the N-terminus of PKDREJ is located extracellularly and can be detected by the anti-PKDREJ antibodies directed against an N-terminal epitope.

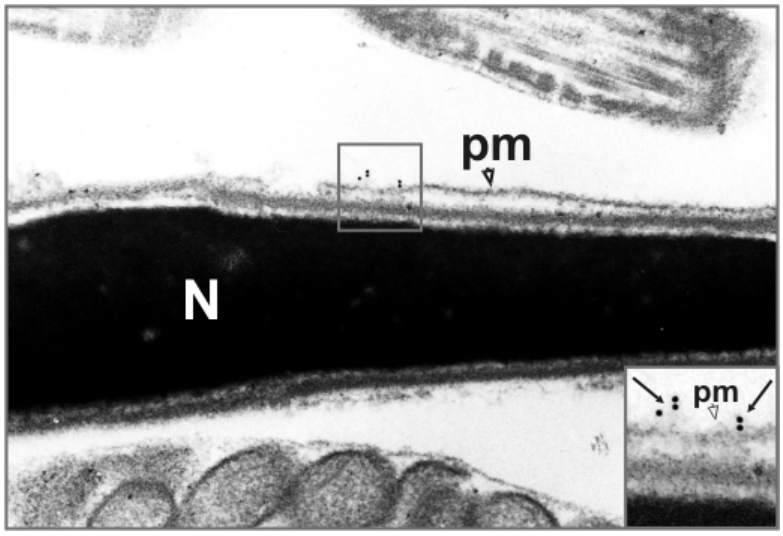

Figure. 4.13. Localization of PKDREJ on the plasma membrane of mouse sperm head
Transmission electron micrograph of ultrathin sections of mouse spermatozoa preincubated with specific PKDREJ antibodies. Secondary goat anti-rabbit IgG were labelled with 10 nm gold. N – nucleus, pm – plasma membrane. Black arrows indicate the location of gold particles (original magnification × 16 700).

Finally, we examined the effect of anti-PKDREJ antibodies on the induction of AR. Capacitated mouse sperm were incubated with anti-PKDREJ antibodies prior to the induction of AR by soluble mouse ZP. As a negative control, we used antibodies against mouse TRPM4, a monovalent selective cation channel that is not expressed in mouse

spermatozoa (data not shown). After a 30-min incubation with buffer 17.6 ± 2 % of sperm were acrosome-reacted (n=3). Incubation with ZP increased this fraction to 29.5 ± 1 %. ZP-induced AR was unaffected by preincubation of sperm with anti-PKDREJ (31.8 ± 2 %) or anti-TRPM4 (31 ± 4 %) antibodies. Likewise, addition of anti-PKDREJ antibodies in the absence of ZP did not significantly increase the fraction of acrosome-reacted sperm (20 ± 3 %). These results, however, cannot exclude a role of PKDREJ for acrosomal exocytosis, because the antibodies used may not have activating or blocking activities.

4.7. Non-testicular PKDREJ expression and localization

Employing the results of this study described above one could suggest that PKDREJ is a germ cells or even sperm-specific protein. The only challenging finding so far was detection of PKDREJ mRNA expression in lung by Northern-blot analysis (see Fig. 4.1.). Since specific PKDREJ antibodies were developed and characterized during this study we took the advantage of immunohistochemical technique to investigate PKDREJ expression in other non-testicular mouse tissues.

4.7.1. Localization of PKDREJ in heat muscle and pulmonary vessels

Cryosections of mouse heart and lung were incubated with the primary anti-PKDREJ antibodies and counterstained with propidium iodide to visualize cell nuclei. In heart we observed specific staining in cardiac muscle cells (Fig. 4.14. A) that was completely blocked by preincubation of antibodies with blocking peptide (Fig. 4.14. C). At a higher magnification confocal thin-section imaging disclosed a regular grid of discrete foci of fluorescence, which represents a prominent transverse tubules (T-tubules) staining pattern (Fig. 4.14. B). In lung tissue we detected the PKDREJ expression exclusively in pulmonary vessels (Fig. 4.15. A). Increasing of magnification revealed the localization of PKDREJ in smooth muscle cells with a grid staining pattern as it was observed in heart (Fig. 4.15. B). Interestingly, the was no signal detected in coronary vessels (Fig. 4.14. A), in aorta smooth muscle cells (Fig. 4.15. D), in skeletal muscles or in blood vessels of any other tissues examined by immunohistochemical approach (testis, epididymis, kidney, liver, duodenum, stomach).

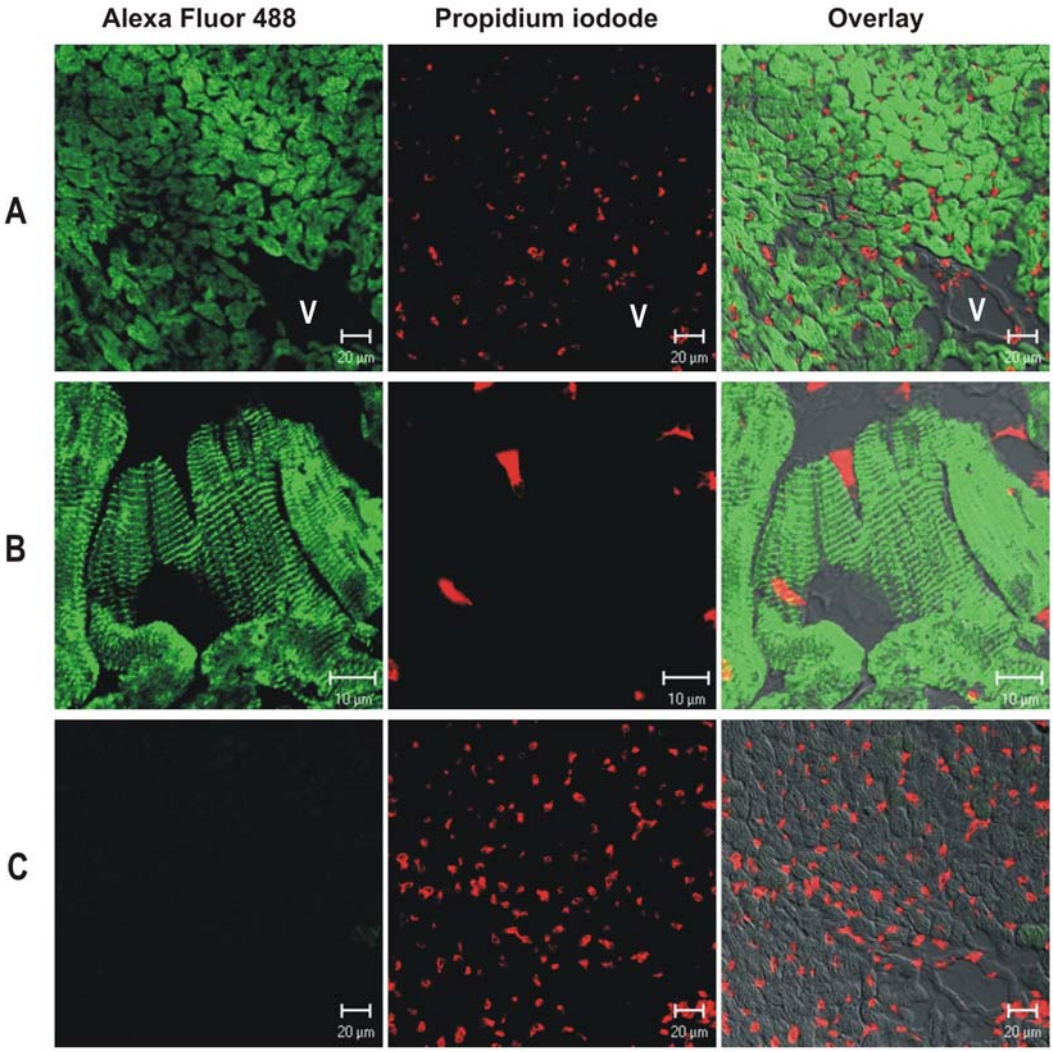

Figure. 4.14. Immunolocalization of PKDREJ in mouse heart

Cryosections of mouse heart **(A, B)** were stained with PKDREJ-specific antibodies (green signal). Cells nuclei were additionally stained with propidium iodide (red signal). Panel **(C)** shows peptide blocking control. Images of Alexa Fluor 488 fluorescence, propidium iodide fluorescence and overlay of both with differential interference contrast images are depicted (scale bars 20µm (A, C) and 10µm (B)). V – coronary blood vessel.

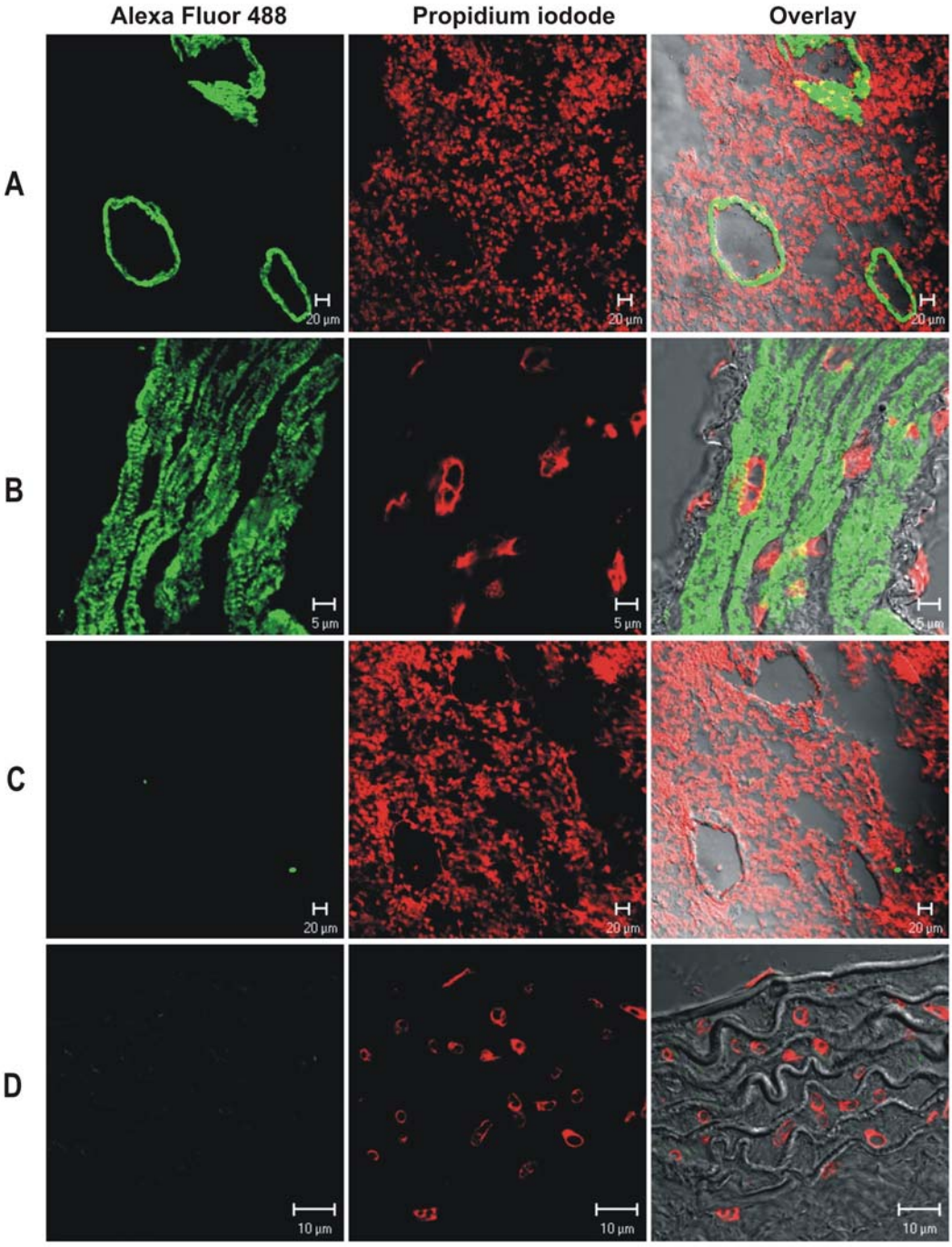

Figure. 4.15. PKDREJ immunolocalization in pulmonary vessels

Cryosections of mouse lung **(A, B)** and aorta **(D)** were stained with PKDREJ-specific antibodies (green signal). Cells nuclei were additionally stained with propidium iodide (red signal). Panel **(C)** shows peptide blocking control in lung tissue. Images of Alexa Fluor 488 fluorescence, propidium iodide fluorescence and overlay of both with differential interference contrast images are depicted (scale bars 20µm (A, C), 10µm (D) and 5µm (B)).

4.7.2. Localization of PKDREJ in primary cilia

Considering that both PKD1 and PKD2 proteins are strongly expressed in kidney and supposed to be important for kidney physiology we were interested whether the PKDREJ is present in kidney tissue also. To this end, indirect immunofluorescence experiments employing anti-PKDREJ antibodies with cryosections of mouse kidney were performed. The signal we observed was localized in epithelial cells of ducts located in cortical part of the organ and was very similar to the staining of primary cilia

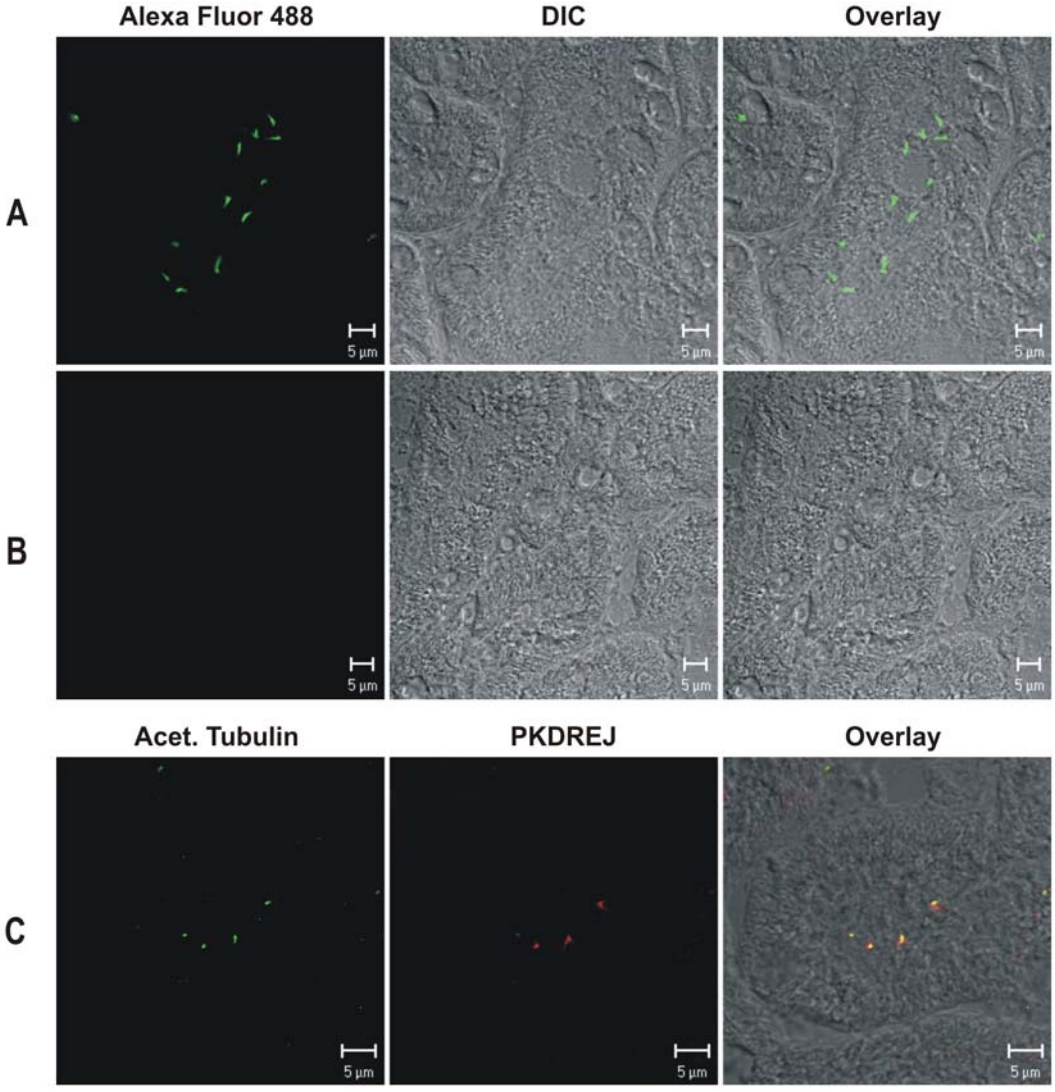

Figure. 4.16. Immunolocalization of PKDREJ in primary cilia of kidney epithelium
Cryosections of mouse kidney **(A)** were stained with PKDREJ-specific antibodies. Panel **(B)** shows peptide blocking control. Images of Alexa Fluor 488 fluorescence, differential interference contrast images (DIC) and overlay of both are depicted. **(C)** Mouse kidney cryosections were stained with antibodies against acetilated tubulin (green signal) and anti-PKDREJ antibodies (red signal). Both stainings and their overlay with corresponding DIC image are schown (scale bars 5µm).

(Fig. 4.16. A). Preincubation of the antibodies with the competing peptide entailed the complete loss of labeling (Fig. 4.16. B). To prove primary cilia localization of PKDREJ in kidney epithelial cells double-staining with antibodies against acetylated α-tubulin, specific ciliary axoneme marker, was performed. Figure 4.16. C displays the result of this experiment where signal corresponding the PKDREJ protein is co-localized with one from acetylated α-tubulin.

Another interesting finding was made while carrying out immunohistochemical examination of epididymis. Epithelial cells in the duct of caput epididymidis displayed typical to primary cilia staining when treated with anti-PKDREJ antibodies (Fig. 4.17. A and B). Such expression pattern was only observed in principal cells of the epididymal duct in caput but not in distal regions of the organ including corpus and cauda.

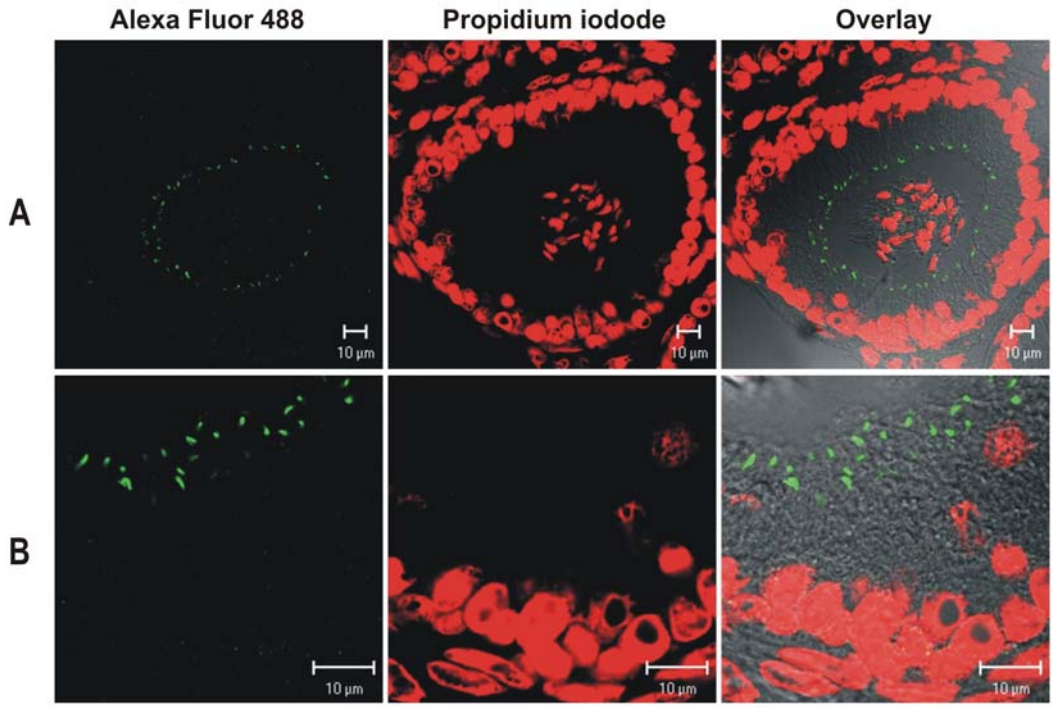

Figure. 4.17. PKDREJ immunolocalization in epithelial cells of caput epididymis

Cryosections of caput epididymis **(A, B)** were stained with PKDREJ-specific antibodies (green signal). Cells nuclei were additionally stained with propidium iodide (red signal). Images of Alexa Fluor 488 fluorescence, propidium iodide fluorescence and overlay of both with corresponding differential interference contrast images are depicted (scale bars 10µm).

5. DISCUSSION

To date, the mammalian polycystin family comprises eight proteins that can further be subdivided into two groups based on their presumptive protein secondary structure. PKD1-like proteins are integral membrane proteins characterized by a large extracellular N-terminus, 11 membrane-spanning regions and a cytoplasmic tail. The extracellular N-terminus contains several structural motifs such as an REJ-domain suggestive of receptor function. The combination of an extracellular GPS and a PLAT/LH2 domain located in the first intracellular loop (s. Fig. 1.3.) are the structural criteria that define these proteins as PKD1 family members (Li et al., 2003). PKD2-like proteins have the structural signature of 6 transmembrane domains with intracellular N- and C-termini and belong to the large superfamily of TRP cation channels (Clapham, 2003; Montell, 2005). Among the PKD1-like proteins, PKDREJ is set apart by a number of characteristic features: Its more than 2000 amino acids are coded on one exon only and its expression is restricted to testis (Hughes et al., 1999). In this study we identified spermatogenic cells as the testicular cell type expressing PKDREJ and demonstrated protein localization on the plasma membrane in the acrosomal region and on the inner aspect of the falciform-shaped sperm head. We provide the first biochemical characterization of PKDREJ and show that it does not undergo cleavage within G-protein-coupled receptor proteolytic site. With generated anti-PKDREJ specific antibodies we could reveal non-testicular PKDREJ expression and localization patterns.

5.1. PKDREJ is a plasma membrane protein of mouse sperm head

Although the PKDREJ gene was identified in 1999, nothing was known about the protein up to now. Its homology to the sea urchin receptor for egg jelly proteins and testis-restricted expression were the only prerequisites for this study. Since the process of mammalian fertilization on the molecular level is still poorly defined PKDREJ has emerged as promising molecularly identified component of the fertilization cascade.

Despite PKDREJ is not incorporated into the plasma membrane of heterologous expression models such as HEK293, COS7, GC-1, GC-2 cells and *Xenopus laevis*

oocytes, we detected the protein in the plasma membrane of mouse sperm. The inability of proteins of being correctly trafficked to the plasma membrane after heterologous expression is a common phenomenon of many sperm proteins especially of those participating in signal transduction processes. We envisage the same scenario for PKDREJ as for the recently identified Ca^{2+}-permeable channels CatSper and CatSper2 (Quill et al., 2001; Ren et al., 2001) which most likely require either sperm-specific adaptor proteins or co-trafficking partners absent in heterologous systems in order to be properly trafficked and functionally active.

There is mounting evidence that signalling proteins such as receptors or ion channels are incorporated into protein complexes and function only in concert with other partner proteins. Thus, it was demonstrated that heterodimerization of PKD1 and PKD2 (TRPP2) facilitates PKD2 translocation to the cell surface where the two proteins form a functional cation channel (Hanaoka et al., 2000). In a similar way, co-expression of PKD2L1 together with PKD1 resulted in trafficking of PKD2L1 channel to the cell surface, whereas expressed alone it was retained within the endoplasmatic reticulum (Murakami et al., 2005). Recently, suREJ3 has been shown to associate with the sea urchin PKD2 homologue and that both proteins localize to the plasma membrane covering the acrosomal vesicle of sea urchin sperm (Neill et al., 2004). Therefore, PKD2L2 which is prominently expressed in testis (Guo et al., 2000), appeared to be a promising interaction partner for PKDREJ. In our hands, however, co-expression of both proteins in HEK293 cells did not affect their subcellular localization: Both proteins were retained intracellularly irrespective of whether they were co-expressed or not. Looking for a probable adaptor protein we tried co-expression of PKDREJ with testis-specific chaperone HspA2 that promotes cytoplasmic extrusion and remodelling of the plasma membrane during spermatogenesis and sperm maturation (Eddy, 1999). In this experiment we did not observe any influence of HspA2 on PKDREJ subcellular distribution in HEK293 cells.

If it were not for our findings with mouse spermatozoa, one might even argue that PKDREJ and PKD2L2 proteins that are expressed in testis serve a role inside the cell. Along these lines, the issue as to whether PKD2 is an intracellular or plasma membrane channel has been surrounded by much controversy (Witzgall, 2005). Recently, two new families of PKD2-interacting proteins have been identified that direct trafficking of the ion channel to distinct subcellular compartments (Hidaka et al., 2004; Kottgen et al.,

2005). Therefore, a systematic search for PKDREJ-interacting proteins in testis should be a rewarding approach to shed light on the mechanisms governing cellular targeting and function of PKDREJ.

PKDREJ has been proposed to play a role in mammalian fertilization similar to that of suREJ proteins, namely to participate in the induction of sperm AR (Mengerink et al., 2000). Being expressed in the plasma membrane of spermatozoa, PKDREJ may function as both a receptor and/or an ion channel in the chain of signaling events leading to acrosomal exocytosis. In this context, suREJ1 binds to the fucose sulphate polymer of egg jelly, thereby eliciting Ca^{2+} influx and eventually AR (Vacquier and Moy, 1997). Like suREJ1, PKDREJ has an extensive extracellular N-terminus that may bind a ligand, participate in cell-cell adhesion or work as a sensor for mechanical stimuli as invoked for PKD1 (Kierszenbaum, 2004). In addition, PKDREJ has a putative pore region may therefore serve as an ion channel. As an initial step to address these issues, we incubated capacitated mouse spermatozoa with our antibodies directed against the PKDREJ N-terminus in order to induce AR. On the other hand we had a try to block ZP3-induced AR by the preincubation of capacitated mouse sperm with the same antibodies. Unfortunately, in both experiments we have not observed antibody-induced Ca^{2+} influx or a significant increase/decrease in the fraction of acrosome-reacted sperm so far. These observations, however, do not exclude a role of PKDREJ for the induction of AR, since the antibodies may not be able to stabilize like a native ligand an active protein conformation required for transmembrane signaling.

An additional twist to the role of PKD family members in the fertilization process provides the recent finding that a *Drosophila* flagellar PKD2 homolog, called amo (for almost there) is localized to the distal tip of the sperm flagella and is specifically expressed in the male germline (Watnick et al., 2003). A targeted mutation of the amo gene causes almost complete sterility. Both the structure of the testis and the characteristics of sperm motility in the amo mutant and the wild-type fly were normal. However, sperm of the mutant deposited in the uterus were unable to enter the female sperm storage organs (seminal receptacles and spermathecae), thus suggesting a sperm storage defect. Supporting a role of PKD2 homolog in *Drosophila* fertilization is the finding by Gao (Gao et al., 2003) that the fly pkd-2 gene, encoding a Ca^{2+}-activated, non-selective channel, expresses a protein associated with the head and tail of sperm. Like in the amo gene mutant, targeted disruption of pkd-2 results in male sterility

without affecting spermatogenesis. Like in the amo mutant, sperm of the pkd-2 mutant are motile but unable to swim into the storage organs of the female. From these data, it appears that pkd-2 cation channel in *Drosophila* plays a critical role in sperm directional movement inside the female reproductive tract.

Likewise, lov-1 (PKD1 homolog) and pkd-2 *C. elegance* mutants exhibit a defect of the male mating behaviour associated with the fault in the sensory system (Kaletta et al., 2003). Male worms are presumed to find hermaphrodites and locate the vulva via chemical cues and sense contact with the sensory rays in the male tail. While wild-type *C. elegance* males are attracted to hermaphrodites and rapidly locate the vulva, males deficient in either or both lov-1 and pkd-2 are dramatically less successful in locating the vulva, resulting in significantly decreased male mating efficiencies. Such supporting fertilization sensory function observed in *Drosophila* and *C. elegance* is one more intriguing possibility where PKDs including PKDREJ can play a role since mammalian sperm as well as sea urchin sperm also move directionally to meet the egg in the oviduct.

In fact, male infertility is observed in patients with ADPKD (van der Linden et al., 1995). The finding in human, sea urchin, *C. elegance* and *Drosophila* of polycystin gene homologs not only provides support to evolutionary conservation but also points to genetically defined components required in the male for fertilization. In addition, the PKD1/PKD2 complex also participates in cell-cell junction and cell-extracellular matrix interactions, which so far have not been defined in wild-type and ADPKD models. Although expression of all known PKD family members can be found in testis (s. Fig. 1.2.), it is still elusive how polycystins operate during testicular organogenesis and maturation and how critical are polycystin protein complexes in mammalian sperm function. These issues may represent a paramount challenge because PKD1 and PKD2 gene products can themselves activate intracellular signaling cascades that regulate cell proliferation, migration, and differentiation. An integration of these pathways, involving G-proteins, phosphorylation of serine kinases and protein kinases, and intracellular second messengers including calcium, may be critical for sperm function. Further studies of mice with targeted mutations of PKD family members (Lu et al., 1997; Wu et al., 1998) or conditional knockout animals in which either gene can be inactivated during adulthood could provide answers to these questions.

5.2. PKDREJ is not cleft at the GPS domain in heterologous expression systems

In our study we provide the first available biochemical data on PKDREJ. Upon heterologous expression in two different systems we did not observe cleavage of PKDREJ at the GPS domain as reported to occur in PKD1 and suREJ3 proteins (Mengerink et al., 2002; Qian et al., 2002). The physiological meaning of GPS cleavage in G-protein coupled receptors and other proteins is still poorly understood. For PKD1 it was demonstrated that cleavage requires not only GPS but also REJ domain and cleavage-disrupting mutations within the latest one facilitate cysts formation. Although cleavage-deficient forms of PKD1 traffic like a wild-type protein to the cell surface, it was shown that mutations impairing cleavage of latrophilin, a G-protein coupled receptor with GPS domain, prevented its delivery to the plasma membrane (Volynski et al., 2004). Interestingly, in all known cases both protein fragments remain associated after cleavage and traffic together but may behave as independent proteins while participating in signal transduction. The interaction between two parts is rather non-covalent since in case of suREJ3 its N-terminus can be removed from the membrane by incubating cells in pH 9.2 filtered seawater (Mengerink et al., 2002).

Amino acid sequence comparisons of GPS domains of proteins already shown to be cleft with that of PKDREJ revealed two noticeable distinctions which may explain disturbance of its cleavage (s. Fig. 1.3. C). Firstly, the highly conserved cleavage motif H L ^ T (where " ^ " indicates the position of cleavage) in both human and mouse PKDREJ contains an additional histidine residue and is present as H L H T. Secondly, two conserved cysteine residues that usually immediately precede the cleavage motif are absent in PKDREJ. These residues can only be found 20 amino acid positions upstream of the predicted cleavage site. According to the paradigm proposed by Lin et al. (Lin et al., 2004), cleavage in the GPS domain is an autocatalytic intramolecular reaction, which does not require the involvement of any cell-specific proteases. Our finding that PKDREJ remains uncleft in two different expression models is fully compatible with the latter assumption. However, the functional relevance of PKDREJ GPS processing or its absence as well as the presence of PKDREJ cleavage in native system still remain to be determined.

5.3. PKDREJ localization in transverse tubules and in primary cilia

Previously, the PKDREJ expression was considered to be restricted to testis what was demonstrated by Northern-blot analysis (Hughes et al., 1999). Although the PKDREJ expression in testis was predominant, by Northern blot we could also detected a weak signal in lung (see Fig. 4.1.). Having PKDREJ-specific antibodies as a tool for immunohistochemical examination we found the protein in some other non-testicular tissues like heart, lung, kidney and epididymis. Among PKD proteins this tissue distribution is rather usual since all other known PKDs are widely expressed with prevalence in heart and kidney (Guo et al., 2000; Li et al., 2003; Murakami et al., 2005; Nomura et al., 1998; Yuasa et al., 2002). However, in comparison with kidney epithelia the physiological role for PKDs presence in other tissues is not well understood.

Investigating non-testicular distribution of PKDREJ we found the protein expression in cardiomyocytes and smooth muscles of pulmonary blood vessels. At that the staining pattern of PKDREJ subcellular localization corresponded to transverse tubules (T-tubules) – invaginations of the sarcolemma with associated glycocalyx which entering the sarcoplasm along the surface of the sarcoplasmic reticulum. T-tubules form a sarcolemmal tubule network of branching tubules with both transverse and longitudinal elements. One consequence of this network of narrow tubules is that a rapid change in the composition of the solution around a ventricular myocyte results in a slower change in the composition of the fluid within the t-tubules because of the time required for diffusion into the t-tubular network (Brette and Orchard, 2003). T-tubules have been suggested to play a central role in excitation-contraction coupling in myocytes. Many of the proteins involved in this process appear to be concentrated within or adjacent to the t-tubule membrane forming complexes or dyads. Ca^{2+}-handling proteins in particular appear to be located predominantly within t-tubules supporting their function as the major site for Ca^{2+} entry and release, allowing synchronous Ca^{2+} release throughout the cell and Ca^{2+} removal form the cytoplasm (Brette and Orchard, 2003). Along these lines, a high density of L-type Ca^{2+} channels in t-tubules was shown (Brandt, 1985; Takagishi et al., 2000) and their coupling with the Ca^{2+}-release channels in sarcoplasmic reticulum (ryanodine receptors, RyRs) was suggested (Carl et al., 1995; Scriven et al., 2000). Some Na^{+}-handling proteins like $Na_{v1.1}$, $Na_{v1.3}$ and $Na_{v1.6}$ are

located predominantly in the t-tubules but their function at the site is still unclear (Maier et al., 2002). There is some evidence that Na^+-Ca^{2+} exchanger (NCX) is present at the t-tubules, however it is still controversial, weather this protein is at a higher concentration in the t-tubules or is homogeneously distributed between the t-tubules and surface sarcolemma (Frank et al., 1992; Kieval et al., 1992; Musa et al., 2002; Scriven et al., 2000). From proteins participating in signalling cascades G_s, adenylate cyclase, and A-kinase anchoring protein were shown to be concentrated at the t-tubule membrane (Gao et al., 1997; Laflamme and Becker, 1999; Yang et al., 1998), and protein phosphatase calcineurin together with protein kinase A were localized near the t-tubules (Santana et al., 2002).

If the signal transduction cascade providing excitation-contraction coupling in cardiomyocytes within t-tubules seems to be well understood, there are still a lot of questions concerning t-tubules function and genesis. What is less clear, how are the t-tubules maintained, and how and why do they change during development, hypertrophy, and heart failure? It is tempting to speculate that members of PKD family could provide further answers to these questions. It is well known that cardiovascular abnormalities are a characteristic feature of ADPKD. They include cerebral aneurysms, hypertension, and cardiac vascular defects. Mice with targeted PKD1 or PKD2 mutations display not only renal but also pancreatic and hepatic failure, and cardiac defects (Boulter et al., 2001; Wu et al., 1998; Wu et al., 2000). Both PKD1 and PKD2 are highly expressed throughout cardiovascular system during embryonic development and in adult organism. Interestingly, by single-cell RT-PCR only expression of PKD2 and PKD2L2 could be detected in ventricular cardiomyocytes whereas PKD1 and PKD1L1 expression appeared to be limited to non-myocyte cardiac tissue (Volk et al., 2003). However, there is no data available concerning subcellular localization of PKD2 or PKD2L2 in cardiomyocytes. In vascular smooth muscle cells it was demonstrated that the expression of PKD1 is developmentally regulated, whereas PKD2 has a more constant level of expression (Qian et al., 2003). Significant co-localization of the PKD1 signal and PKD2 signal was found in vascular smooth muscles cells kept in primary culture but most of the staining seemed to be cytoplasmic, consistent with much of the protein being located intracellularly, possibly in vesicles and sarcoplasmic reticulum. These observations are consistent with an important role of polycystins in the development, maintenance, and function of cardiovascular system, despite the molecular

mechanisms involved must be further investigated as well as new adequate models have to be proposed.

As it was already mentioned the function of polycystins is mainly investigated in kidney where both PKD1 and PKD2 can be found and co-localized in primary cilia of renal epithelial cells (Nauli et al., 2003). Therefore it was not a surprise to detect PKDREJ located in kidney epithelium in primary cilia, although its role in this tissue and particularly in this cell organelle still needs to be determined. Primary cilia are thin hair like structures that typically appear as single projection from one of the two basal bodies (centrioles). Although they have been observed for decades, their functions are not known. Some hypotheses were proposed concerning the importance of primary cilia in renal function as well as body axis asymmetry. The multiple kidney cysts were the first indication of a relationship between the primary cilium and polycystic kidney disease. It was noticed that mice with mutations in PKD2 have, in addition to the polycystic phenotype, abnormal left-right development (Pennekamp et al., 2002). It is somehow connected to the expression of PKD2 in nodal cilia during embryonic development but the clear mechanism of the left-right asymmetry body formation is not understood .

Schwartz and co-workers showed that primary cilia of cultured renal cells were able to bend, when the cells were superfused at flow rates comparable to these seen in renal tubules (Schwartz et al., 1997). Measurements of the degree of bending detected that the strain on the ciliary membrane must be larger on the convex side of the bent cilium. A link between the cilium deformation and cell signaling provides the observation that intracellular Ca^{2+} concentration increased in response to changes in the flow rate (Praetorius and Spring, 2001). Interestingly, only the initial part of this signal transduction event requires Ca^{2+} influx and this influx is not sensitive to blockers of voltage-gated Ca^{2+} channels, but is inhibited by Gd^{3+} and amiloride. Recent evidence shows that the Ca^{2+}-permeable channel involved in flow sensing is PKD2 (Nauli et al., 2003), although a connection between mechanosensation and cyst formation as seen in polycystic kidney disease is purely speculative (Praetorius and Spring, 2005). Other data obtained from PKD1 and PKD2 deficient cells suggest that the sensing of the fluid flow might be important for maintaining cell polarization. In *C. elegans* it was demonstrated that primary cilia are essential for chemo- and osmosensation. Mutations that affect the structure of the cilia resulted in sensory defects such as altered osmotic

avoidance, poor mating behaviour, and defective chemotaxia (Apfeld and Kenyon, 1999). In mammalian the kidney primary cilia seem to be important for the regulation of fluid composition. In renal distal tubule, an increase in luminal flow rate is known to induce K^+ secretion and increase the lumen-negative transepithelial potential differences (Malnic et al., 1989). During this study we also observed PKDREJ staining in cilia of epithelial cells orientated into the lumen of caput but not cauda epididymis. Interestingly, most of the fluid discharged from testis with spermatozoa is absorbed within the caput part, thus regulating ion balance and increasing sperm concentration (Clulow et al., 1994). Further studies have to be done to answer questions whether PKDREJ expressed in primary cilia contributes in mechanical, chemo- or osmosensation and in which signal transduction pathways this protein is involved.

5.4. Conclusions, implications and perspectives

Spermatozoa are highly differentiated, polarized and compartmentalized cells with the sole function to fuse with the egg in order to create a new unique entity. Although they are a part of a multicellular organism, their physiology is completely different from somatic cells. Therefore, closer understanding of male gametes functioning is so important not only for reproductive biology and medicine but also for fundamental life science. In the present study we investigated a new protein, PKDREJ, and provided the first data about its structure, expression and localization. We were able to demonstrate that PKDREJ is highly expressed in testicular tissue and localized on the plasma membrane in the acrosomal region and on the inner aspect of the falciform-shaped mouse sperm head. Since PKDREJ gene is evolutionary conservative among species, it is tempting to assume its important role in spermatozoa physiology and function.

Furthermore, PKDREJ is a member of a relatively new polycystin protein family, which members are most likely involved in various types of cellular sensing. Two of them PKD1 and PKD2 are also responsible for the development of autosomal-dominant polycystic kidney disease. This makes the whole family very interesting from a medical point of view, since the pathophysiology of the disease remains elusive. Along these lines, we provided the first evidence of non-testicular PKDREJ expression, detecting the protein in transverse tubules of cardiomyocytes and in primary cilia of renal and epididymal epithelial cells. These data open a new field of research for understanding

the function of PKDREJ, which will aid in assessing the physiological relevance of its PKD1-like homologs including the proteins responsible for polycystic kidney disease. As exemplified its sea urchin homologs, further biochemical, cell biological and functional studies on PKDREJ have the potential to provide deeper insight into the molecular mechanisms of mammalian fertilization.

6. SUMMARY

The mammalian polycystic kidney disease (PKD) gene family comprises eight members whose role in cell physiology is still poorly understood. Two of the founding members of the family, PKD1 and PKD2, are responsible for the majority of cases of autosomal dominant polycystic kidney disease. While PKD1 is considered to be a cell-surface receptor, PKD2 functions as a cation channel and has been described both at the plasma membrane and intracellularly. The present study focuses on PKDREJ – polycystic kidney disease and receptor for egg jelly, a protein that contains both a large receptor-like extracellular part and a putative ion channel region. PKDREJ homology to suREJ proteins, which seem to play a role in the induction of the sperm acrosome reaction in sea urchin, gives a reason to propose the same scenario for PKDREJ in mammals. Although the PKDREJ gene was identified in 1999, its features and protein characteristics remained elusive up to now.

The present study investigates mouse PKDREJ gene and protein and provides the first data about its structure, expression and localization. It demonstrates that PKDREJ is highly expressed in testicular tissue and its expression there is restricted to germ cells and spermatozoa.

Upon heterologous expression in HEK 293, COS7, GC-1, GC-2 cells and *Xenopus laevis* oocytes PKDREJ is retained intracellularly in endoplasmatic compartments. Since many known receptors and ion channels can not be properly trafficked without special partner or adaptor proteins, while expressed in a heterologous system, co-expression experiments with mouse HspA2, PKD2L2 and human PKD1 and PKD2 were done. In all cases PKDREJ localization remained intracellular irrespective of whether it was co-expressed with other proteins or not.

The presence of the GPS domain in the PKDREJ amino acid structure gave a reason to speculate about the proteolytical cleavage within this site. The present work provides not only the biochemical characterisation of the PKDREJ protein, but also the first evidence about lack of the GPS processing. It shows that PKDREJ unlike PKD1 or

suREJ3 does not undergo cleavage within G-protein-coupled receptor proteolytic site while being expressed in HEK293 cells or *Xenopus laevis* oocytes. Moreover, the explanation of this phenomenon, based on the structure of the GPS domain in PKDREJ and the autocatalytic mechanism of the cleavage, is proposed.

To investigate the PKDREJ protein in native system PKDREJ-specific polyclonal antibodies were developed and characterised. By means of indirect immunofluorescence it was possible to demonstrate PKDREJ localization in the acrosomal region and on the inner aspect of the falciform-shaped mouse sperm head. Additional immunoelectron microscopy with mouse sperm revealed the plasma membrane localization of the PKDREJ protein and confirmed the predicted protein topology with the N-terminus located extracellularly.

To examine the functional relevance of PKDREJ in terms of the induction of the sperm acrosome reaction capacitated mouse sperm was incubated with antibodies directed against the PKDREJ N-terminus. We have not observed antibody-induced Ca^{2+} influx or a significant increase in the fraction of acrosome-reacted sperm. Also, anti-PKDREJ antibodies failed to block ZP-induced acrosome reaction. These observations do not completely exclude a role of PKDREJ for the induction of the acrosome reaction, since the antibodies may neither be able to stabilize an active protein conformation required for transmembrane signaling nor to block relevant epitopes needed for ZP signaling. However, it may be also the first hint for another role of PKDREJ in sperm physiology.

Although all other PKD family members are widely expressed, PKDREJ expression was considered to be testis-specific. Investigating non-testicular tissue distribution of PKDREJ we were able to detect the protein in cardiomyocytes and smooth muscles of pulmonary blood vessels; the staining pattern of PKDREJ subcellular localization in both cell types corresponded to transverse tubules (t-tubules). Another site of non-testicular expression was discovered in epithelial cells of kidney and epididymis. In kidney epithelium PKDREJ was co-localized with acetylated α-tubulin, a marker of primary cilia. These results open a new direction for the further

investigation of PKDREJ that will provide deeper insight into its function and physiological relevance.

7. ZUSAMMENFASSUNG

Die *polycystic kidney disease* (PKD)-Genfamilie besteht aus acht Genen, deren Rolle in der Zellphysiologie weiterhin zum größten Teil unklar ist. Die zwei zuerst entdeckten Mitglieder dieser Familie, PKD1 und PKD2, sind für die meisten Fälle der autosomal dominanten polyzystischen Nierenerkrankung verantwortlich. Während PKD1 ein zellmembranständiger Rezeptor zu sein scheint, handelt es sich bei PKD2 um einen Kationenkanal, welcher sowohl in der Zellmembran als auch intrazellulär beschrieben wurde. Die vorliegende Studie fokussiert auf *polycystic kidney disease and receptor for egg jelly* (PKDREJ), ein Protein welches sowohl einen großen rezeptorähnlichen extrazellulären Teil als auch einen mutmaßlichen Ionenkanal beinhaltet. Die Homologie von PKDREJ zu *sea urchin receptor for egg jelly* (suREJ)-Proteinen, welche wahrscheinlich eine Rolle in der Induktion der akrosomalen Reaktion von Spermatozoen bei Seeigeln spielen, gibt Anlass zu der Spekulation, dass PKDREJ die gleiche Funktion bei Säugetieren erfüllt. Obwohl das PKDREJ-Gen schon 1999 entdeckt wurde, sind seine Eigenschaften und Proteinmerkmale bislang weitestgehend unklar.

Diese Studie untersucht das murine PKDREJ-Gen und -Protein und beschreibt erstmalig dessen Struktur, Expression und Lokalisation. Es wird gezeigt, dass PKDREJ stark in testikulärem Gewebe exprimiert wird und diese Expression auf Keimzellen und Spermatozoen beschränkt ist.

Nach heterologer Expression in HEK 293-, COS7-, GC-1- und GC-2-Zellen sowie in *Xenopus laevis*-Eizellen verbleibt PKDREJ intrazellulär in endoplasmatischen Kompartimenten. Da viele bekannte Rezeptoren und Ionenkanäle, ohne spezielle Partner- oder „Adaptor“-Proteine nicht bestimmungsgemäß transportiert werden, wenn man sie in heterologen Systemen exprimiert, wurden Koexpressions-Experimente mit murinem HspA2, einem testisspezifischen Chaperon, PKD2L2, einem PKD2 eng verwandten Ionenkanal, und menschlichem PKD1 und PKD2 durchgeführt. In allen Fällen verblieb PKDREJ intrazellulär, unabhängig davon, ob mit oder ohne Koexpression anderer Proteine.

Das Vorhandensein einer GPS-Domäne in der PKDREJ-Aminosäuresequenz gab Anlass, die proteolytische Spaltung in dieser Region zu untersuchen. Dabei charakterisiert diese Arbeit nicht nur biochemische Eigenschaften des PKDREJ-Proteins, sondern gibt auch erste Hinweise auf eine fehlende proteolytische Abspaltung der N-terminalen Proteindomäne. In HEK293-Zellen oder *Xenopus laevis*-Oozyten exprimiertes PKDREJ wird im Gegensatz zu PKD1 oder suREJ3 nicht in seiner GPS-Domäne gespalten. Außerdem wird eine Erklärung dieses Phänomens, basierend auf der Struktur der GPS-Domäne von PKDREJ und dem autokatalytischem Mechanismus der Spaltung, vorgeschlagen.

Um das PKDREJ-Protein in einem nativen System zu untersuchen, wurden PKDREJ-spezifische polyklonale Antikörper entwickelt und charakterisiert. Durch indirekte Immunofluoreszenz war es möglich, PKDREJ in der akrosomalen Region und am inneren Anteil des sichelförmigen murinen Spermienkopfes zu lokalisieren. Zusätzliche Immun-Elektronenmikroskopie mit murinen Spermien zeigte die Lokalisation des PKDREJ-Proteins in der Plasmamembran und sicherte die vorausgesagte Protein-Topologie mit einem extrazellulär liegenden N-Terminus.

Um die funktionelle Relevanz von PKDREJ in Hinblick auf die Induktion der akrosomalen Reaktion zu zeigen wurden kapazitierte murine Spermien mit Antikörpern gegen das N-terminale Ende von PKDREJ-Protein inkubiert. Wir konnten keinen antikörperinduzierten Ca^{2+}-Einstrom oder eine signifikante Steigerung des Anteils akrosomreagierter Spermien beobachten. Des weiteren blockierten anti-PKDREJ Antikörper die *Zona pellucida* (ZP)-induzierte akrosomale Reaktion nicht. Diese Beobachtungen schließen eine Rolle von PKDREJ in der Akrosomreaktion nicht vollständig aus, da die Antikörper eventuell nicht in der Lage sind, eine aktive Proteinkonformation, eine Voraussetzung für die transmembranäre Signalkette, zu stabilisieren oder die relevanten Epitope, die für ZP-Signaltransduktion benötigt werden, zu blockieren. Dennoch könnte diese Arbeit der erste Hinweis einer anderen, noch unbekannten Funktion von PKDREJ in der Physiologie von Spermien sein.

Obwohl die Mitglieder der PKD-Familie vielerorts exprimiert werden, galt PKDREJ bislang als hodenspezifisch. Wir konnten auf Proteinebene PKDREJ allerdings in Herzmuskelzellen und Lungenblutgefäßen nachweisen, wobei das Färbemuster von PKDREJ in beiden Zelltypen auf eine Lokalisation an den transversen Tubuli schließen lässt. Weitere nicht-testikuläre Expression wurde in Nierenepithelzellen und im Epididymis entdeckt. Im Nierenepithel war PKDREJ mit acetyliertem α-Tubilin kolokalisiert, einem Marker von primären Zilien. Diese Resultate bilden die Grundlage für weiterführende Untersuchungen zur Funktion und physiologischen Relevanz von PKDREJ.

8. REFERENCES

Amann, R. P., and Howards, S. S. (1980). Daily spermatozoal production and epididymal spermatozoal reserves of the human male. *J Urol* **124,** 211-5.

Apfeld, J., and Kenyon, C. (1999). Regulation of lifespan by sensory perception in Caenorhabditis elegans. *Nature* **402,** 804-9.

Barr, M. M., and Sternberg, P. W. (1999). A polycystic kidney-disease gene homologue required for male mating behaviour in C. elegans. *Nature* **401,** 386-9.

Boatman, D. E., and Robbins, R. S. (1991). Bicarbonate: carbon-dioxide regulation of sperm capacitation, hyperactivated motility, and acrosome reactions. *Biol Reprod* **44,** 806-13.

Boulter, C., Mulroy, S., Webb, S., Fleming, S., Brindle, K., and Sandford, R. (2001). Cardiovascular, skeletal, and renal defects in mice with a targeted disruption of the Pkd1 gene. *Proc Natl Acad Sci U S A* **98,** 12174-9.

Brandt, N. (1985). Identification of two populations of cardiac microsomes with nitrendipine receptors: correlation of the distribution of dihydropyridine receptors with organelle specific markers. *Arch Biochem Biophys* **242,** 306-19.

Brette, F., and Orchard, C. (2003). T-tubule function in mammalian cardiac myocytes. *Circ Res* **92,** 1182-92.

Carl, S. L., Felix, K., Caswell, A. H., Brandt, N. R., Ball, W. J., Jr., Vaghy, P. L., Meissner, G., and Ferguson, D. G. (1995). Immunolocalization of sarcolemmal dihydropyridine receptor and sarcoplasmic reticular triadin and ryanodine receptor in rabbit ventricle and atrium. *J Cell Biol* **129,** 672-82.

Chen, H., and Sampson, N. S. (1999). Mediation of sperm-egg fusion: evidence that mouse egg alpha6beta1 integrin is the receptor for sperm fertilinbeta. *Chem Biol* **6,** 1-10.

Clapham, D. E. (2003). TRP channels as cellular sensors. *Nature* **426,** 517-24.

Clulow, J., Jones, R. C., and Hansen, L. A. (1994). Micropuncture and cannulation studies of fluid composition and transport in the ductuli efferentes testis of the rat: comparisons with the homologous metanephric proximal tubule. *Exp Physiol* **79,** 915-28.

Coronel, C. E., and Lardy, H. A. (1987). Characterization of Ca^{2+} uptake by guinea pig epididymal spermatozoa. *Biol Reprod* **37,** 1097-107.

Delmas, P. (2004). Polycystins: from mechanosensation to gene regulation. *Cell* **118,** 145-8.

Eddy, E. M. (1999). Role of heat shock protein HSP70-2 in spermatogenesis. *Rev Reprod* **4,** 23-30.

Forssmann, W. G., Ito, S., Weihe, E., Aoki, A., Dym, M., and Fawcett, D. W. (1977). An improved perfusion fixation method for the testis. *Anat Rec* **188,** 307-14.

Frank, J. S., Mottino, G., Reid, D., Molday, R. S., and Philipson, K. D. (1992). Distribution of the Na(+)-Ca^{2+} exchange protein in mammalian cardiac myocytes: an immunofluorescence and immunocolloidal gold-labeling study. *J Cell Biol* **117,** 337-45.

Fraser, L. R. (1987). Minimum and maximum extracellular Ca^{2+} requirements during mouse sperm capacitation and fertilization in vitro. *J Reprod Fertil* **81,** 77-89.

Fraser, L. R. (1995). Cellular biology of capacitation and the acrosome reaction. *Hum Reprod* **10 Suppl 1,** 22-30.

Galindo, B. E., Moy, G. W., and Vacquier, V. D. (2004). A third sea urchin sperm receptor for egg jelly module protein, suREJ2, concentrates in the plasma membrane over the sperm mitochondrion. *Dev Growth Differ* **46,** 53-60.

Gao, T., Puri, T. S., Gerhardstein, B. L., Chien, A. J., Green, R. D., and Hosey, M. M. (1997). Identification and subcellular localization of the subunits of L-type calcium channels and adenylyl cyclase in cardiac myocytes. *J Biol Chem* **272,** 19401-7.

Gao, Z., Ruden, D. M., and Lu, X. (2003). PKD2 cation channel is required for directional sperm movement and male fertility. *Curr Biol* **13,** 2175-8.

Go, K. J., and Wolf, D. P. (1985). Albumin-mediated changes in sperm sterol content during capacitation. *Biol Reprod* **32,** 145-53.

Guo, L., Schreiber, T. H., Weremowicz, S., Morton, C. C., Lee, C., and Zhou, J. (2000). Identification and characterization of a novel polycystin family member, polycystin-L2, in mouse and human: sequence, expression, alternative splicing, and chromosomal localization. *Genomics* **64,** 241-51.

Hanaoka, K., Qian, F., Boletta, A., Bhunia, A. K., Piontek, K., Tsiokas, L., Sukhatme, V. P., Guggino, W. B., and Germino, G. G. (2000). Co-assembly of polycystin-1 and -2 produces unique cation-permeable currents. *Nature* **408,** 990-4.

Hidaka, S., Konecke, V., Osten, L., and Witzgall, R. (2004). PIGEA-14, a novel coiled-coil protein affecting the intracellular distribution of polycystin-2. *J Biol Chem* **279,** 35009-16.

Hofmann, M. C., Hess, R. A., Goldberg, E., and Millan, J. L. (1994). Immortalized germ cells undergo meiosis in vitro. *Proc Natl Acad Sci U S A* **91,** 5533-7.

Hofmann, M. C., Narisawa, S., Hess, R. A., and Millan, J. L. (1992). Immortalization of germ cells and somatic testicular cells using the SV40 large T antigen. *Exp Cell Res* **201,** 417-35.

Hughes, J., Ward, C. J., Aspinwall, R., Butler, R., and Harris, P. C. (1999). Identification of a human homologue of the sea urchin receptor for egg jelly: a polycystic kidney disease-like protein. *Hum Mol Genet* **8,** 543-9.

Johnson, L., and Varner, D. D. (1988). Effect of daily spermatozoan production but not age on transit time of spermatozoa through the human epididymis. *Biol Reprod* **39,** 812-7.

Jones, R. C. (1999). To store or mature spermatozoa? The primary role of the epididymis. *Int J Androl* **22,** 57-67.

Jungnickel, M. K., Marrero, H., Birnbaumer, L., Lemos, J. R., and Florman, H. M. (2001). Trp2 regulates entry of Ca^{2+} into mouse sperm triggered by egg ZP3. *Nat Cell Biol* **3,** 499-502.

Kaletta, T., Van der Craen, M., Van Geel, A., Dewulf, N., Bogaert, T., Branden, M., King, K. V., Buechner, M., Barstead, R., Hyink, D., Li, H. P., Geng, L., Burrow, C., and Wilson, P. (2003). Towards understanding the polycystins. *Nephron Exp Nephrol* **93,** e9-17.

Kierszenbaum, A. L. (2004). Polycystins: what polycystic kidney disease tells us about sperm. *Mol Reprod Dev* **67,** 385-8.

Kieval, R. S., Bloch, R. J., Lindenmayer, G. E., Ambesi, A., and Lederer, W. J. (1992). Immunofluorescence localization of the Na-Ca exchanger in heart cells. *Am J Physiol* **263,** C545-50.

Kottgen, M., Benzing, T., Simmen, T., Tauber, R., Buchholz, B., Feliciangeli, S., Huber, T. B., Schermer, B., Kramer-Zucker, A., Hopker, K., Simmen, K. C., Tschucke, C. C., Sandford, R., Kim, E., Thomas, G., and Walz, G. (2005). Trafficking of TRPP2 by PACS proteins represents a novel mechanism of ion channel regulation. *Embo J* **24,** 705-16.

Laemmli, U. K. (1970). Cleavage of structural proteins during the assembly of the head of bacteriophage T4. *Nature* **227,** 680-5.

Laflamme, M. A., and Becker, P. L. (1999). G(s) and adenylyl cyclase in transverse tubules of heart: implications for cAMP-dependent signaling. *Am J Physiol* **277,** H1841-8.

Lee, M. A., and Storey, B. T. (1986). Bicarbonate is essential for fertilization of mouse eggs: mouse sperm require it to undergo the acrosome reaction. *Biol Reprod* **34,** 349-56.

Li, A., Tian, X., Sung, S. W., and Somlo, S. (2003). Identification of two novel polycystic kidney disease-1-like genes in human and mouse genomes. *Genomics* **81,** 596-608.

Lin, H. H., Chang, G. W., Davies, J. Q., Stacey, M., Harris, J., and Gordon, S. (2004). Autocatalytic cleavage of the EMR2 receptor occurs at a conserved G protein-coupled receptor proteolytic site motif. *J Biol Chem* **279,** 31823-32.

Lin, Y., Mahan, K., Lathrop, W. F., Myles, D. G., and Primakoff, P. (1994). A hyaluronidase activity of the sperm plasma membrane protein PH-20 enables sperm to penetrate the cumulus cell layer surrounding the egg. *J Cell Biol* **125,** 1157-63.

Lu, W., Peissel, B., Babakhanlou, H., Pavlova, A., Geng, L., Fan, X., Larson, C., Brent, G., and Zhou, J. (1997). Perinatal lethality with kidney and pancreas defects in mice with a targetted Pkd1 mutation. *Nat Genet* **17,** 179-81.

Maier, S. K., Westenbroek, R. E., Schenkman, K. A., Feigl, E. O., Scheuer, T., and Catterall, W. A. (2002). An unexpected role for brain-type sodium channels in coupling of cell surface depolarization to contraction in the heart. *Proc Natl Acad Sci U S A* **99,** 4073-8.

Malnic, G., Berliner, R. W., and Giebisch, G. (1989). Flow dependence of K+ secretion in cortical distal tubules of the rat. *Am J Physiol* **256,** F932-41.

Mengerink, K. J., Moy, G. W., and Vacquier, V. D. (2000). suREJ proteins: new signalling molecules in sea urchin spermatozoa. *Zygote* **8 Suppl 1,** S28-30.

Mengerink, K. J., Moy, G. W., and Vacquier, V. D. (2002). suREJ3, a polycystin-1 protein, is cleaved at the GPS domain and localizes to the acrosomal region of sea urchin sperm. *J Biol Chem* **277,** 943-8.

Montell, C. (2005). The TRP superfamily of cation channels. *Sci STKE* **2005,** re3.

Moy, G. W., Mendoza, L. M., Schulz, J. R., Swanson, W. J., Glabe, C. G., and Vacquier, V. D. (1996). The sea urchin sperm receptor for egg jelly is a modular protein with extensive homology to the human polycystic kidney disease protein, PKD1. *J Cell Biol* **133,** 809-17.

Murakami, M., Ohba, T., Xu, F., Shida, S., Satoh, E., Ono, K., Miyoshi, I., Watanabe, H., Ito, H., and Iijima, T. (2005). Genomic organization and functional analysis of murine PKD2L1. *J Biol Chem* **280,** 5626-35.

Musa, H., Lei, M., Honjo, H., Jones, S. A., Dobrzynski, H., Lancaster, M. K., Takagishi, Y., Henderson, Z., Kodama, I., and Boyett, M. R. (2002). Heterogeneous expression of Ca(2+) handling proteins in rabbit sinoatrial node. *J Histochem Cytochem* **50,** 311-24.

Nauli, S. M., Alenghat, F. J., Luo, Y., Williams, E., Vassilev, P., Li, X., Elia, A. E., Lu, W., Brown, E. M., Quinn, S. J., Ingber, D. E., and Zhou, J. (2003). Polycystins 1

and 2 mediate mechanosensation in the primary cilium of kidney cells. *Nat Genet* **33,** 129-37.

Neill, A. T., Moy, G. W., and Vacquier, V. D. (2004). Polycystin-2 associates with the polycystin-1 homolog, suREJ3, and localizes to the acrosomal region of sea urchin spermatozoa. *Mol Reprod Dev* **67,** 472-7.

Neill, A. T., and Vacquier, V. D. (2004). Ligands and receptors mediating signal transduction in sea urchin spermatozoa. *Reproduction* **127,** 141-9.

Neill, J. M., and Olds-Clarke, P. (1987). A computer-assisted assay for mouse sperm hyperactivation demonstrates that bicarbonate but not bovine serum albumin is required. *Gamete Res* **18,** 121-40.

Nomura, H., Turco, A. E., Pei, Y., Kalaydjieva, L., Schiavello, T., Weremowicz, S., Ji, W., Morton, C. C., Meisler, M., Reeders, S. T., and Zhou, J. (1998). Identification of PKDL, a novel polycystic kidney disease 2-like gene whose murine homologue is deleted in mice with kidney and retinal defects. *J Biol Chem* **273,** 25967-73.

O'Toole, C. M., Arnoult, C., Darszon, A., Steinhardt, R. A., and Florman, H. M. (2000). Ca(2+) entry through store-operated channels in mouse sperm is initiated by egg ZP3 and drives the acrosome reaction. *Mol Biol Cell* **11,** 1571-84.

Pennekamp, P., Karcher, C., Fischer, A., Schweickert, A., Skryabin, B., Horst, J., Blum, M., and Dworniczak, B. (2002). The ion channel polycystin-2 is required for left-right axis determination in mice. *Curr Biol* **12,** 938-43.

Praetorius, H. A., and Spring, K. R. (2001). Bending the MDCK cell primary cilium increases intracellular calcium. *J Membr Biol* **184,** 71-9.

Praetorius, H. A., and Spring, K. R. (2005). A physiological view of the primary cilium. *Annu Rev Physiol* **67,** 515-29.

Primakoff, P., and Myles, D. G. (2002). Penetration, adhesion, and fusion in mammalian sperm-egg interaction. *Science* **296,** 2183-5.

Qian, F., Boletta, A., Bhunia, A. K., Xu, H., Liu, L., Ahrabi, A. K., Watnick, T. J., Zhou, F., and Germino, G. G. (2002). Cleavage of polycystin-1 requires the receptor for egg jelly domain and is disrupted by human autosomal-dominant polycystic kidney disease 1-associated mutations. *Proc Natl Acad Sci U S A* **99,** 16981-6.

Qian, Q., Li, M., Cai, Y., Ward, C. J., Somlo, S., Harris, P. C., and Torres, V. E. (2003). Analysis of the polycystins in aortic vascular smooth muscle cells. *J Am Soc Nephrol* **14,** 2280-7.

Quill, T. A., Ren, D., Clapham, D. E., and Garbers, D. L. (2001). A voltage-gated ion channel expressed specifically in spermatozoa. *Proc Natl Acad Sci U S A* **98,** 12527-31.

Rankin, T. L., Tong, Z. B., Castle, P. E., Lee, E., Gore-Langton, R., Nelson, L. M., and Dean, J. (1998). Human ZP3 restores fertility in Zp3 null mice without affecting order-specific sperm binding. *Development* **125,** 2415-24.

Ren, D., Navarro, B., Perez, G., Jackson, A. C., Hsu, S., Shi, Q., Tilly, J. L., and Clapham, D. E. (2001). A sperm ion channel required for sperm motility and male fertility. *Nature* **413,** 603-9.

Reynolds, E. S. (1963). The use of lead citrate at high pH as an electron opaque stain in electron microscopy. *J Cell Biol* **17,** 208.

Ruknudin, A., and Silver, I. A. (1990). Ca^{2+} uptake during capacitation of mouse spermatozoa and the effect of an anion transport inhibitor on Ca^{2+} uptake. *Mol Reprod Dev* **26,** 63-8.

Santana, L. F., Chase, E. G., Votaw, V. S., Nelson, M. T., and Greven, R. (2002). Functional coupling of calcineurin and protein kinase A in mouse ventricular myocytes. *J Physiol* **544,** 57-69.

Schwartz, E. A., Leonard, M. L., Bizios, R., and Bowser, S. S. (1997). Analysis and modeling of the primary cilium bending response to fluid shear. *Am J Physiol* **272,** F132-8.

Scriven, D. R., Dan, P., and Moore, E. D. (2000). Distribution of proteins implicated in excitation-contraction coupling in rat ventricular myocytes. *Biophys J* **79,** 2682-91.

Takagishi, Y., Yasui, K., Severs, N. J., and Murata, Y. (2000). Species-specific difference in distribution of voltage-gated L-type Ca(2+) channels of cardiac myocytes. *Am J Physiol Cell Physiol* **279,** C1963-9.

Toshimori, K. (2003). Biology of spermatozoa maturation: an overview with an introduction to this issue. *Microsc Res Tech* **61,** 1-6.

Turner, T. T. (1995). On the epididymis and its role in the development of the fertile ejaculate. *J Androl* **16,** 292-8.

Vacquier, V. D., and Moy, G. W. (1997). The fucose sulfate polymer of egg jelly binds to sperm REJ and is the inducer of the sea urchin sperm acrosome reaction. *Dev Biol* **192,** 125-35.

van der Linden, E. F., Bartelink, A. K., Ike, B. W., and van Leeuwaarden, B. (1995). Polycystic kidney disease and infertility. *Fertil Steril* **64,** 202-3.

Visconti, P. E., Bailey, J. L., Moore, G. D., Pan, D., Olds-Clarke, P., and Kopf, G. S. (1995a). Capacitation of mouse spermatozoa. I. Correlation between the capacitation state and protein tyrosine phosphorylation. *Development* **121,** 1129-37.

Visconti, P. E., Moore, G. D., Bailey, J. L., Leclerc, P., Connors, S. A., Pan, D., Olds-Clarke, P., and Kopf, G. S. (1995b). Capacitation of mouse spermatozoa. II. Protein tyrosine phosphorylation and capacitation are regulated by a cAMP-dependent pathway. *Development* **121,** 1139-50.

Volk, T., Schwoerer, A. P., Thiessen, S., Schultz, J. H., and Ehmke, H. (2003). A polycystin-2-like large conductance cation channel in rat left ventricular myocytes. *Cardiovasc Res* **58,** 76-88.

Volynski, K. E., Silva, J. P., Lelianova, V. G., Atiqur Rahman, M., Hopkins, C., and Ushkaryov, Y. A. (2004). Latrophilin fragments behave as independent proteins that associate and signal on binding of LTX(N4C). *Embo J* **23,** 4423-33.

Ward, C. R., and Storey, B. T. (1984). Determination of the time course of capacitation in mouse spermatozoa using a chlortetracycline fluorescence assay. *Dev Biol* **104,** 287-96.

Watnick, T. J., Jin, Y., Matunis, E., Kernan, M. J., and Montell, C. (2003). A flagellar polycystin-2 homolog required for male fertility in *Drosophila*. *Curr Biol* **13,** 2179-84.

Witzgall, R. (2005). Polycystin-2-an intracellular or plasma membrane channel? *Naunyn Schmiedebergs Arch Pharmacol*.

Wu, G., D'Agati, V., Cai, Y., Markowitz, G., Park, J. H., Reynolds, D. M., Maeda, Y., Le, T. C., Hou, H., Jr., Kucherlapati, R., Edelmann, W., and Somlo, S. (1998). Somatic inactivation of Pkd2 results in polycystic kidney disease. *Cell* **93,** 177-88.

Wu, G., Markowitz, G. S., Li, L., D'Agati, V. D., Factor, S. M., Geng, L., Tibara, S., Tuchman, J., Cai, Y., Park, J. H., van Adelsberg, J., Hou, H., Jr., Kucherlapati, R., Edelmann, W., and Somlo, S. (2000). Cardiac defects and renal failure in mice with targeted mutations in Pkd2. *Nat Genet* **24,** 75-8.

Yanagimachi, R. (1984). Fertilization in mammals. *Tokai J Exp Clin Med* **9,** 81-5.

Yanagimachi, R. (1994). Mammalian fertilization. *In* "The physiology of reproduction." (E. N. Knobil, JD, Ed.), pp. 189-317. New York: Raven Press.

Yang, J., Drazba, J. A., Ferguson, D. G., and Bond, M. (1998). A-kinase anchoring protein 100 (AKAP100) is localized in multiple subcellular compartments in the adult rat heart. *J Cell Biol* **142,** 511-22.

Yuan, R., Primakoff, P., and Myles, D. G. (1997). A role for the disintegrin domain of cyritestin, a sperm surface protein belonging to the ADAM family, in mouse sperm-egg plasma membrane adhesion and fusion. *J Cell Biol* **137,** 105-12.

Yuasa, T., Venugopal, B., Weremowicz, S., Morton, C. C., Guo, L., and Zhou, J. (2002). The sequence, expression, and chromosomal localization of a novel

polycystic kidney disease 1-like gene, PKD1L1, in human. *Genomics* **79,** 376-86.

9. ABBREVIATIONS

ADPKD	Autosomal dominant polycystic kidney disease
AR	Acrosome reaction
bp	Base pair
BSA	Bovine serum albumin
cDNA	Complementary DNA
CFP	Cyan fluorescent protein
DEPC	Diethylpyrocarbonate
DMEM	Dulbecco's modified Eagle medium
DMSO	Dimethylsulfoxide
DNA	Desoxyribonucleic acid
DTT	Dithiothreitol
ECL	Enhanced chemiluminescence
EDTA	Etylendiamine tetraacedic acid
FCS	Fetal calf serum
FITC	Fluoresceinisothiocyanate
GalT	Galactosyl transferase
GC	Germ cells
GPCR	G-protein coupled receptor
GPS	G-protein coupled receptor proteolytic site
GST	Glutathion-S-transferase
Hsp	Heat shock protein
IPTG	Isopropyl-beta-D-thiogalactopyranoside
kb	Kilobase
kDa	Kilodalton
LB	Luria-Bertani
ORF	Open reading frame
PBS	Phosphate-buffered saline
PCR	Polymerase chain reaction
PKD	Polycystic kidney disease
PKDREJ	Polycystic kidney disease and receptor for egg jelly

PLAT/LH	Polycystin-1, Lipoxygenase, Alpha-Toxin / Lipoxygenase homology
RNA	Ribonucleic acid
SDS	Sodium dodecyl sulfate
suREJ	Sea urchin receptor for egg jelly
TAE	Tris/acetate/EDTA
TRP	Transient receptor potential
YFP	Yellow fluorescence protein
ZP	Zona pellucida

10. ACKNOWLEDGEMENTS

I would like to thank Prof. Dr. Thomas Gudermann for accepting my thesis project and for giving me the opportunity to achieve my PhD under his supervision.

Foremost, I would like to thank Dr. Vladimir Chubanov for introducing me to my project and for teaching me a great deal about science. I am very appreciative for his encouragement, his enthusiasm for science and for always having an open ear for me.

I am also grateful to all members of DFG Graduate Seminar "Cell-Cell Interaction in Reproduction" for helpful discussions, and especially Prof. Dr. Gerhard Aumüller and Dr. Klaus Steger for giving me the chance to accomplish some parts of this thesis in their laboratories.

I would like to thank my laboratory colleagues for all their help, especially Alexander Dietrich, Thomas Hofmann, Thomas Büch, Silke Kaske, Hermann Kalwa, Dorke Meyer and last but not least Tanja Pfeffer-Eckel.

Finally, I thank my parents and my German family who always supported my endeavour with love, humor and generosity. Nothing in my career would have ever been possible without them.

11. CURRICULUM VITAE

Personal data

Name:	Yulia Butscheid née Gantievskaya
Date of birth:	October 8, 1978
Place of birth:	Minsk, Belarus
Citizenship:	Republic of Belarus
Marital status:	Married

Address

Paumgartner Straße 15
90429 Nürnberg
Germany

Education

09/1985-07/1991	Comprehensive school # 37, Minsk, Belarus
09/1991-07/1993	Pedagogic gymnasium, Minsk, Belarus
09/1993-07/1995	Belarusian State University lyceum with university-entrance diploma, Minsk, Belarus

Academic education and scientific work

09/1995-08/2000	International Sakharov Environmental University, Minsk, Belarus
07/2000	State examination in Immunology & Environmental Medicine

08/2000	Diploma in Radiobiology & Environmental Medicine
10/2000-11/2003	Post-graduate study, International Sakharov Environmental University, Minsk, Belarus
08/2002-07/2005	DFG Graduate Seminar "Cell-cell interaction in reproduction", Marburg, Germany
08/2002-09/2005	PhD student with Prof. Dr. Thomas Gudermann at the Institute of Pharmacology and Toxicology, Philipps-University Marburg, Marburg, Germany

Work experience

10/1997-06/2000	Scientific laboratory assistant in the Belarusian bone marrow transplantation centre, Minsk, Belarus
08/2000-06/2001	Web-designer, Design ME Ltd, Minsk, Belarus
08/2001-10/2002	Director, Medi-Plus Ltd., PCR-diagnostic of infectious diseases, Minsk, Belarus
since 10/2005	Clinical research associate, Novartis Pharma GmbH, Nuernberg

12. PUBLICATIONS

12.1. Original publications generated within the scope of the thesis

Butscheid Y, Chubanov V, Steger K, Meyer D, Dietrich A, Gudermann T. 2005. Polycystic kidney disease and receptor for egg jelly is a plasma membrane protein of mouse sperm head. Mol Reprod Dev. 2006 Mar;73(3):350-60.

12.2. Contributions to congresses

Gantievskaya Y, Chubanov V, Dietrich A, Gudermann T.
Ca^{2+}- signaling in sperm.
7. Dies Andrologicus und 3. Kongress des Graduiertenkollegs "Zell-Zell-Interaktion im Reproduktionsgeschehen", Marburg, 2003

Gantievskaya Y, Chubanov V, Dietrich A, Steger K, Gudermann T.
Expression and localization of mPKDREJ in mouse testis and sperm.
45. Frühjahrstagung der Deutschen Gesellschaft für experimentelle und klinische Pharmakologie und Toxikologie, Mainz, 2004

Gantievskaya Y, Chubanov V, Kaske S, Dietrich A, Gudermann T.
TRP channels in sperm.
4^{th} Congress of the DFG-Graduate Seminar, Giessen, 2004

Gantievskaya Y, Chubanov V, Steger K, Dietrich A, Gudermann T.
Polycystic kidney disease and receptor for egg jelly is a plasma membrane protein of mouse sperm head.
38^{th} Annual Meeting of the Society for the Study of Reproduction, Quebec City, 2005

13. AKADEMISCHE LEHRER

Meine akademischen Lehrer waren die Damen und Herren in Minsk:

Baikov, Bartkevich, Batyan, Bokut, Chistik, Chudakov, Figurin, Goncharova, Gritsai, Gurachevskiy, Gutko, Homenko, Kapitula, Karpovich, Kiselev, Kovaleva, Kovkova, Lapko, Lavrinenko, Lobanok, Loiko, Lutsko, Melnov, Merkulova, Milyutin, Mishatkina, Miskevich, Mosse, Naumenko, Novikova, Obolonkin, Piven, Potapnev, Romanovskaya, Rogov, Savanovich, Sautkina, Seliavko, Shavlov, Sheiko, Sholuh, Sychev, Tolstaya, Yurin und Zafranskaya;

in Marburg:
Aumüller, Gudermann und Krause;

in Giessen:
Bergmann, Hinsch, Hoffmann und Meinhardt.

14. EHRENWÖRTLICHE ERKLÄRUNG

Ich erkläre ehrenwörtlich, dass ich die dem Fachbereich Medizin Marburg zur Promotionsprüfung eingereichte Arbeit mit dem Titel: „Characterization of mouse polycystic kidney disease and receptor for egg jelly gene and protein in heterologous and native system“ im Institut für Pharmakologie und Toxikologie der Philipps-Universität Marburg unter Leitung von Prof. Dr. T. Gudermann mit Unterstützung durch Dr. V. Chubanov ohne sonstige Hilfe selbst durchgeführt und bei der Abfassung der Arbeit keine anderen als die in der Dissertation angeführten Hilfsmittel benutzt habe.

Ich habe bisher an keinem in- und ausländischen medizinischen Fachbereich ein Gesuch um Zulassung zur Promotion eingereicht noch die vorliegende oder eine andere Arbeit als Dissertation vorgelegt.

Teile der vorliegenden Arbeit wurde im Molecular Reproduction and Development (Mol Reprod Dev. 2006 Mar;73(3):350-60.) veröffentlicht.

(Yulia Butscheid) Marburg, den 15. Dezember 2005